



# Modelling root exudation and plant-microbe interactions under CO<sub>2</sub> fertilization in a mature forest

Kristian Schufft<sup>1,2,3</sup>, Katrin Fleischer<sup>4</sup>, Anja Rammig<sup>3</sup>, Lin Yu<sup>5</sup>, Mingkai Jiang<sup>6</sup>, Belinda E. Medlyn<sup>7</sup>, Sönke Zaehle<sup>1,8</sup>

5 <sup>1</sup> Department Biogeochemical Signals, Max Planck Institute for Biogeochemistry, Jena, Germany

<sup>2</sup> International Max Planck Research School for Global Biogeochemical Cycles, Max Planck Institute for Biogeochemistry, Jena, Germany

<sup>3</sup> Technical University of Munich, School of Life Sciences, Freising, Germany

10 <sup>4</sup> Systems Ecology, Amsterdam Institute for Life and Environment, Vrije Universiteit Amsterdam, Amsterdam, The Netherlands

<sup>5</sup> Department of Earth System Sciences, Hamburg University, Hamburg, Germany

<sup>6</sup> State Key Laboratory for Vegetation Structure, Function and Construction (VegLab), College of Life Sciences, Zhejiang University, Hangzhou, Zhejiang, China, 310030

<sup>7</sup> Hawkesbury Institute for the Environment, Western Sydney University, Penrith NSW Australia

15 <sup>8</sup> Michael Stifel Center Jena for Data-driven and Simulation Science, Friedrich Schiller University Jena, Jena, Germany

*Correspondence to:* Kristian Schufft ([kschufft@bgc-jena.mpg.de](mailto:kschufft@bgc-jena.mpg.de))



**Abstract.** Root exudation, defined as labile carbon (C) allocation into soils through fine roots, is a substantial yet often overlooked pathway of the terrestrial carbon cycle. Root exudation is likely to increase under rising levels of atmospheric CO<sub>2</sub>, but the implications of the increase in this flux are poorly understood. Increased labile C availability in soils may stimulate microbial growth and increase soil carbon storage but at the same time microbial nutrient acquisition could offset this accumulation by enhanced decomposition of soil organic matter

Here, we implement a dynamic representation of root exudation based on plant surplus carbon and nutrient limitation in the microbial explicit terrestrial biosphere model QUINCY-JSM (QUantifying Interactions between terrestrial Nutrient CYcles and the climate system). We evaluate the effect of elevated CO<sub>2</sub> on root exudation and its consequences for microbial C, nitrogen (N) and phosphorus (P) cycling using observations from the Eucalyptus Free Air CO<sub>2</sub> Enrichment (EucFACE) experiment in a soil phosphorus impoverished forest. In the experiment, more than half of additional gross primary productivity (GPP) under elevated CO<sub>2</sub> (eCO<sub>2</sub>) could not be assigned to a measured vegetation flux.

With the explicit implementation of root exudation, our model predicted that elevated CO<sub>2</sub> caused an increase in belowground carbon flux and an increase in microbial growth, but a limited effect on soil carbon storage. Root exudation was increased to 30 %, but more than half of this additional input was directly respired by microbes. As a result, root exudation gives a possible explanation for the not measured vegetation flux and the enhanced heterotrophic respiration under eCO<sub>2</sub> observed in the experiment. Increased C input through root exudation also enhanced microbial growth, but in order to support this growth, microbes mostly gained nutrients from decomposition and mineralization of organic matter. As a consequence, increased decomposition negated build-up of microbial necromass. Our study emphasizes the role of root exudation and microbial activity for soil carbon sequestration under elevated CO<sub>2</sub> and guides further research regarding plant-microbe interactions.

**Short summary.** Root exudation describes a process in which plants allocate labile carbon through roots into soils, thereby influencing microbial carbon and nutrient cycling. We implemented root exudation in a computer model that simulates ecosystem processes. Increased atmospheric CO<sub>2</sub> led to increased root exudation, but the additional input was partially offset by enhanced microbial respiration. Our research brings new perspectives in modelling soil carbon and nutrient cycling in forests under increasing CO<sub>2</sub>.



## 1 Introduction

Increasing atmospheric CO<sub>2</sub> concentrations have the potential to drive increased ecosystem carbon sequestration, but there is considerable uncertainty about how much additional C can be stored, particularly where soil nutrient availability is low. CO<sub>2</sub> fertilization leads to higher leaf-level photosynthesis and biomass production (BP) (Norby et al., 2005; Walker et al., 2019, 2021), potentially increasing C sequestration in biomass, and in soils when biomass turn over. However, increased growth must be supported by nutrients and if soil nutrient availability cannot meet increased plant nutrient demands, the CO<sub>2</sub> fertilization effect on plant growth is typically reduced (Fleischer et al., 2019; Norby et al., 2010; Zaehle et al., 2014). ). Soil nutrient availability is thus a major determinant of whether CO<sub>2</sub> fertilization leads to a positive effect on carbon sequestration in biomass. Nonetheless, additional carbon sequestration can occur in soils under nutrient limitation: allocation of C towards mycorrhizae (Drake et al., 2011) and root exudation has been observed to increase in some studies (Norby et al., 2024; Phillips et al., 2011) to support additional nutrient acquisition, and this belowground carbon allocation may induce additional soil carbon storage. Therefore, plant nutrient availability for growth may affect if CO<sub>2</sub> fertilization has a positive effect on carbon sequestration via allocation towards biomass production or induce soil carbon sequestration, via increased belowground allocation.

A critical question for C sequestration under elevated CO<sub>2</sub> (eCO<sub>2</sub>) and nutrient-limited conditions is how much of the extra C allocated belowground remains as organic carbon in the soil system, or is quickly re-emitted to the atmosphere via respiration. The ultimate fate of the C allocated belowground is shaped by an interplay of microbial growth, decomposition, and nitrogen (N) and phosphorus (P) availability. On the one hand, soil microbial organisms are a key driver in soil organic matter cycling as they decompose and take up organic material to gain C, N and P, thereby respiring CO<sub>2</sub> and mineralizing N and P, making them plant-available again. At the same time, their necromass contributes substantially to soil organic C, N and P stocks through organo-mineral associations (Liang et al., 2019). Under additional labile C input four competing mechanisms regulate soil C sequestration:

(i) Inputs of low molecular weight compounds, such as root exudates, may increase microbial growth. However, the amount of C that can be incorporated in microbial biomass depends on microbial nutrient availability. Under microbial nutrient stress a higher fraction of plant-derived C will be directly respired, while under sufficient nutrient availability, microbial biomass C will increase (Manzoni et al., 2012; Spohn, 2015).

(ii) Increased microbial growth can promote microbial necromass formation (Cotrufo et al., 2013). Although microbial necromass is a readily-available source of C, energy and nutrients, microbial biomolecules also are often stabilized through formation of aggregates or sorption to mineral soil matrix, making them inaccessible for enzymatic degradation and contributing to long-term C storage (Kästner et al., 2021; Liang et al., 2017; Sokol et al., 2019). Hence, increased microbial growth induced by additional C inputs has the potential to increase soil organic carbon, and enhance long-term ecosystem C storage.



(iii) On the other hand, increased microbial growth can lead to higher microbial demands for N and P. Microbial necromass represents a source for growth that is rich in N and P. Therefore, increased microbial growth induced by additional C inputs may also induce high microbial demand for nutrients and a shift towards an increased depolymerization and respiration of old organic material (van Groenigen et al., 2014; Vestergård et al., 2016; Yin et al., 2013). This mechanism, often described as priming, has the potential to offset the accumulation of C in soil organic matter (SOM) and thereby increase soil carbon turnover. During this process the enhanced decomposition will increase biological gross mineralization of N and P.

(iv) Additional feedback comes into play under P limitation. Microbes and plants may use biochemical mineralization to acquire P (Margalef et al., 2017; Turner et al., 2014; Walker and Syers, 1976). In this process, P is mobilized via phosphatase enzymes that cleave terminal P from organic compounds (McGill and Cole, 1981; Nannipieri et al., 2011). In contrast to regular biological mineralization, this pathway does not require a complete decomposition of organic material and has therefore no direct influence on soil C cycling. Whether increased root exudation under eCO<sub>2</sub> will lead to an increase in soil C storage therefore depends on the interaction, quantity and nature of microbial growth and nutrient acquisition.

Free Air CO<sub>2</sub> enrichment (FACE) experiments allow to study the effect of elevated CO<sub>2</sub> on plant C allocation and SOM cycling on ecosystem scale, including the advantages of inclusion of mature trees, natural climate conditions and low disturbances (McLeod and Long, 1999). In previous FACE experiments, namely Duke FACE and ORNL FACE, which were located in temperate N-limited forests, eCO<sub>2</sub> has led to an initial increase in NPP. However, the effect persisted only in Duke FACE and diminished in ORNL after 10 years (Norby et al., 2010; Walker et al., 2019). At Duke FACE a stronger increase in N uptake and change in plant nitrogen-use-efficiency allowed for a sustained response in NPP to eCO<sub>2</sub>, while in ORNL FACE where progressive N limitation decreased the response of NPP under eCO<sub>2</sub> (Finzi et al., 2007; Zaehle et al., 2014). One explanation points to increased belowground C allocation in Duke FACE, causing an increase in SOM cycling and therefore enhanced plant nitrogen availability via priming (Drake et al., 2011).

To clarify and quantify the interactions between C and nutrients under rising atmospheric CO<sub>2</sub>, model-data synthesis can be used, bringing together measurements from FACE experiments and terrestrial biosphere models (TBM). Model-data synthesis for FACE experiments identified C allocation, nitrogen uptake and soil nitrogen cycling as key processes for CO<sub>2</sub> responses under N limitation (De Kauwe et al., 2014; Zaehle et al., 2014). However, most models were unable to fully reproduce the dissimilar responses to eCO<sub>2</sub> under nitrogen limitation. While the initial increase in NPP could be reproduced, models generally tend to show decreased response in NPP due to progressing N limitation (Zaehle et al., 2014). One possible explanation is the missing representation of root exudation and priming effects, that would allow plants to acquire nutrients via increased belowground C allocation. Further model development showed that including priming effects based on increased litter and root exudation or representation of mycorrhiza fungi, improved simulated N availability and NPP response for Duke FACE for first order decomposition soil models (Grant, 2013; Thurner et al., 2024). Although the results highlight the role of soil organic matter cycling for plant growth, they paid little attention to the microbial mechanisms and P cycle interactions that affect soil C sequestration under elevated CO<sub>2</sub>.



To further investigate the competing dynamics of microbial growth and nutrient acquisition on soil C storage under eCO<sub>2</sub> we use the terrestrial biosphere model QUINCY-JSM, which accounts for C, N, and P dynamics and explicitly represents the effect of microbial processes that shape soil C cycling (Thum et al., 2019; Yu et al., 2020). We parameterize and apply our model to the Eucalyptus Free Air CO<sub>2</sub> Enrichment (EucFACE) facility (Crous et al., 2015; Ellsworth et al., 2017). EucFACE is of particular relevance because it is the first large scale FACE experiment investigating the impact of eCO<sub>2</sub> on forest ecosystems under P limitation. Despite the fact that P limitation is widespread P globally previous forest FACE experiments have been principally conducted in N-limited temperate forests (Du et al., 2020). Similar to N-limited systems, root exudation is an important mechanism for plant P acquisition (Lambers, 2022; Pantigoso et al., 2023; Reichert et al., 2022) and is likely to increase under enhanced P limitation (De Andrade et al., 2022; Wang and Lambers, 2020) or eCO<sub>2</sub>.

Field measurements and model-data synthesis for EucFACE highlight the importance of root exudation for plant C allocation and P cycling under eCO<sub>2</sub>. At the site eCO<sub>2</sub> led to a 12 % increase of gross primary productivity (GPP), but the effect on biomass production and autotrophic respiration was comparatively small. Notably, more than 50 % of surplus GPP under eCO<sub>2</sub> could not be attributed to a measured vegetation flux in this experiment (Jiang et al., 2020). Instead, this C was traced to an 17 % increase in heterotrophic soil respiration, without a statistically significant increase in soil C. Jiang et al. (2020) hypothesized that increase in heterotrophic respiration to be related to additional C input via root exudation, potentially for nutrient acquisition. However, eCO<sub>2</sub> did only invoke weak effects on plant P availability, suggesting that despite increased belowground C allocation, microbial competition for nutrients constrain additional plant P uptake (Jiang et al., 2024b) Model-data synthesis was done before and during the experiment: (Medlyn et al., 2016) found that response of NPP to eCO<sub>2</sub> was related to model nutrient cycling assumptions: In models with integrated P cycle, under eCO<sub>2</sub> plant uptake remained unchanged, preventing a strong response in NPP to eCO<sub>2</sub>, whereas in other models eCO<sub>2</sub> increased NPP up to 20 %. However, uncertainties arise from P acquisition strategies plants might use under increased C supply (Reichert et al., 2022). Jiang et al. (2024a) compared 8 TBMs, including QUINCY-JSM, to the experimental results of EucFACE, and further pointed to the lack of representation of trade mechanisms between plant C allocation and nutrient availability. As most other models, QUINCY-JSM, allocated additional plant C in either autotrophic respiration, growth or storage but not in heterotrophic respiration. This disagrees with observations and indicates a missing representation of nutrient acquisition strategies and plant-microbe interactions in these models. A substantial part of the ecosystem response of EucFACE to eCO<sub>2</sub> lies in plant-microbe interactions and how their alteration affects soil carbon cycling, which cannot be captured by models yet.

Here we aim to address a key missing link between belowground C allocation and nutrient cycling by implementing dynamic root exudation. We modelled root exudation based on plant fine root respiration and nutrient status. We define root exudation as the combined flux of labile carbon and nitrogen through free exudation, rhizodeposition and loss via mycorrhiza. The explicit representation of microbial processes in QUINCY-JSM allows to decompose the CO<sub>2</sub> effect on soil C sequestration in distinct mechanisms. Therefore, we can assess how increased root exudation under eCO<sub>2</sub> influences soil C storage as a result of competing effects of microbial growth and nutrient acquisition:



1) We first analyze how much of the additional C input is used for microbial growth and how much is matched by increased  
145 heterotrophic respiration.

2) Additional microbial growth will increase microbial nutrient demand. We therefore investigate the sources of additional, N  
and P and quantify the amounts released by decomposition of microbial necromass and by biochemical mineralization.

3) In order to assess the net effect of eCO<sub>2</sub> on soil storage we investigate the simultaneous build up and decomposition of  
microbial necromass and evaluate whether increased root exudation leads to accelerated turnover of soil pools.

150 Simulation results are compared with data from the EucFACE experiment. We conclude our study by presenting key aspects  
in which linking models with field measurements can be used to further improve understanding of plant-soil interactions under  
increasing levels of CO<sub>2</sub>.

## 2 Material and Methods

### 2.1 Overview of modelled processes in QUINCY

155 QUINCY-JSM has two components, a terrestrial biosphere model (QUINCY, (Thum et al., 2019)) coupled to the integrated  
Jena Soil model (JSM, (Yu et al., 2020)) and simulates coupled ecosystem N, P, C and water dynamics (Fig. 1 for an overview).  
In the following sections we first summarize key processes represented in QUINCY and JSM, before introducing the new root  
exudation module.

QUINCY simulates the function of vegetation, which is described by five structural pools (leaves, fine roots, coarse roots,  
160 sapwood and heartwood) and three non-structural pools (labile, storage and fruits) that all contain C, N, and P. Photosynthesis  
is calculated after Friend and Kiang (2005) along a vertical canopy gradient (Kull and Kruijt, 1998), with photosynthetic  
activity assumed proportional to leaf nitrogen content, but attenuated in the presence of sink limitation on growth (Thum et  
al., 2019). Acquired C is added to the labile pool, from which it is used to cover the cost for respiration. Maintenance respiration  
is calculated for each tissue based on tissue N content and temperature (Lloyd and Taylor, 1994). In addition QUINCY accounts  
165 for growth respiration (Atkin et al., 2014) and nutrient uptake respiration (Zerihun et al., 1998). The remaining C in the labile  
pool is then used for, root exudation, growth, storage (Fig. 1 upper panel). N and P taken up by plant roots, or recycled from  
senescing tissues are added to the labile pool. Excess labile C, N and P are stored in a reserve pool, from where these elements  
can be retrieved to buffer low levels of the labile pool, e.g., to ensure the regrowth of foliage and roots, root exudation (Sect.  
2.3) and structural components at the start of the growing season. Upon senescence of structural pools, a fixed fraction of  
170 nutrients is recycled and returned into the labile pool. The remaining biomass (C, N, P) enters the soil via litterfall in form of  
three litter pools (soluble, polymeric, wood). Vegetation and soil processes are calculated at 30 min time-step. All physical  
and biogeochemical soil processes are modelled for 15 discrete soil layers, with exponentially increasing depth and a minimum  
layer depth of 6.5 cm. The model accounts for differences in vegetation by twelve plant functional types (PFTs), of which for  
this study we use only the dry broadleaved evergreen type to represent vegetation at the site.



## 175 2.2 Overview of modelled processes in JSM

Soil biogeochemistry is modelled by a microbially explicit and vertically resolved SOM model ( JSM ,(Yu et al., 2020), Fig. 1 lower panel). All biogeochemical soil pools and processes are modelled for 15 discrete soil layers, along a vertical soil gradient. Soil layer thickness increases exponentially with depth. JSM considers five different SOM pools: dissolved organic matter (DOM), microbial biomass, microbial residues, and organo-mineral associated DOM and microbial residues (Table 1).

180 Depolymerization, DOM uptake and associated biological nutrient mineralization, and inorganic nutrients uptake are affected by the abundance of microbial biomass, either modelled by using forward Michaelis-Menten or reverse Michaelis-Menten kinetics (Schimel and Weintraub, 2003). Microbes take up carbon from DOM (Fig. 1, process 1). Nutrients are acquired from DOM or by immobilization of soluble nutrients (Fig. 1, process 2). DOM taken by microbes either enters microbial biomass or becomes mineralized, based on element-specific use-efficiencies. Carbon-use efficiency of the microbial biomass varies as

185 a function of nutrient availability between 30 % and 50 %, mimicking a change in microbial decomposer community. Mineralized C is emitted from soil as heterotrophic respiration. Soil organic matter and inorganic forms of nutrients are transported between soil layers via water transport (for nutrients and dissolved organic matter) and bioturbation. Microbial decay is modelled as first order decay with a constant turnover time of ~150 days. Dead microbial biomass is partitioned into DOM and microbial residue, corresponding to microbial necromass (Fig. 1, process 3). The fraction of N and P entering DOM

190 is higher than for C, to represent the lower C-to-nutrient ratio in cytoplasm (Schimel and Weintraub, 2003). Additionally, a constant fraction of N is transferred into inorganic soluble pools to mimic grazing on living microbial biomass (Wutzler et al., 2022) (Eq. A1 to A5, Table A2). Decomposition of soluble and woody litter follows first order decay, whereas the depolymerization of polymeric litter (Fig. 1, process 4a) and microbial residue (Fig. 1, process 4b) into DOM is a function of microbial biomass pool and in addition varying enzyme allocation based on microbial nutrient status (Wutzler et al., 2017; Yu et al., 2020). Organo-mineral associated DOM and residue pool are protected from depolymerisation, but are exchanged with the ‘free’ DOM/ residue pool via first-order sorption kinetics (Fig. 1, process 5). Soil solution  $\text{NH}_4$  and  $\text{PO}_4$  are in adsorption/desorption interaction with soil surfaces, simulated by Langmuir equilibrium (Yu et al., 2023). Adsorption, plant uptake and microbial uptake of soluble nutrients are in direct competition with each other (Tang and Riley, 2013). In addition to biological nutrient mineralization that results from microbial DOM uptake,  $\text{PO}_4$  further mobilized through biochemical

200 mineralization via acid phosphatase (Fig. 1, process 6). Biochemical mineralization is regulated by the production of phosphatase, which is assumed to be affected by root and microbial biomass, as well as the C allocation for productions of other enzymes. This process allows for an additional pathway of access to P from microbial residue and both organo-mineral associated pools that cannot be directly depolymerised. As biochemical mineralization does not need complete decomposition of organic substance, it can affect the stoichiometry of target pools. Biochemical mineralization is assumed to be controlled

205 by temperature/moisture and the C: P stoichiometry of the target pools.

New N enters the system via deposition and asymbiotic N fixation (Fig. 1, process 7) and is lost by gaseous emission and lateral loss. New P enters the systems via atmospheric deposition and weathering from parent material, which is controlled by



abiotic and biotic factors. On the other hand, P is made irreversibly unavailable by occlusion or leaves the system by lateral loss.

210

**Table 1: Summary of soil pools in QUINCY-JSM, their turnover times and soil pools they represent.**

Pool in Quincy-JSM	Turnover time	Associated soil pools
<b>Soil organic matter (SOM)</b>		
‘free’ DOM	emergent	DOM/POM
Mineral associated dissolved organic matter (asDOM)	emergent	MAOM
microbes	150 d	Microbial biomass
Microbial necromass		
Microbial residue	emergent	DOM/POM
Mineral associated microbial residue (asRes)	emergent	MAOM
<b>Litter pools</b>		
soluble	30 d	litter
polymeric	emergent	litter
woody	2.5 yr	litter



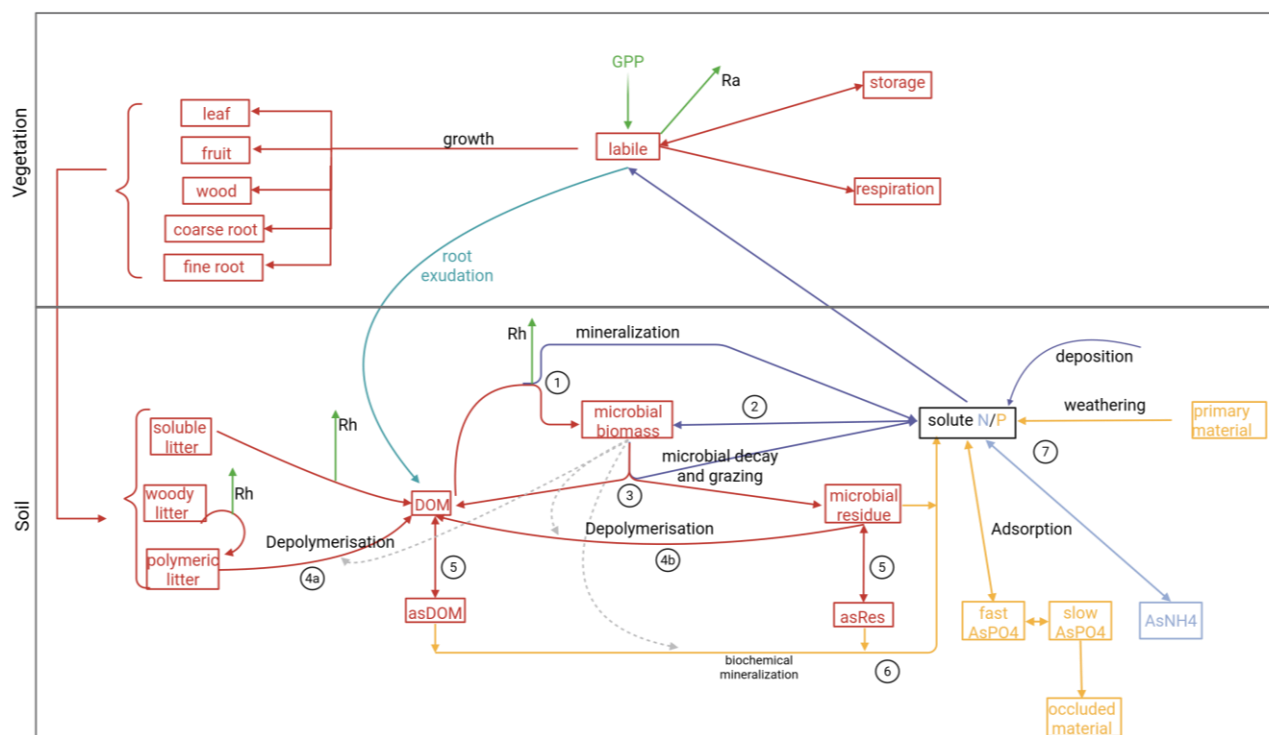


Figure 1: Conceptual scheme of plant-soil interactions and soil processes in Quincy-JSM. Gross primary productivity determines carbon uptake by plants. Organic C, N and P can enter the soil via litterfall and root exudation (C and N). Root litterfall and root exudation can enter deeper soil layers, while other litterfall is added to the topsoil layer. Boxes represent pools and solid arrows fluxes. All soil pools and fluxes are simulated for each soil layer. Dashed arrows represent indirect influence of processes by microbes via enzyme allocation. Red arrows represent fluxes of C, N and P. Green arrows represent C only fluxes (heterotrophic respiration, C uptake). Violet arrows represent N and P fluxes. Yellow: only P fluxes; blue: only N fluxes. Modified from Yu et al. (2020). Created with BioRender.com

### 2.3 New implementation of dynamic root exudation in QUINCY-JSM

To improve the representation of soil-microbe interactions in QUINCY-JSM, we implemented a root exudation module (Fig. 2). Root exudation is modelled as direct, respiration-free flux from the plant labile pool to the soil DOM pool, with a C: N stoichiometry corresponding to the current C: N ratio of the labile pool (Fig. 1). We assume that there is no exudation of P. Implementation of root exudation thus reduces the C and N available for tissue growth and storage and thereby respiration despite no change in the respiration calculations. From the DOM pool, the possible pathways for root exudates are: direct consumption by microbes, adsorption towards the mineral surface or leaching.

The rate of root exudation [ $\text{gC m}^{-2} \text{s}^{-1}$ ] is modelled as a function of fine root respiration [ $\text{gC m}^{-2} \text{s}^{-1}$ ] and plant nutrient status (Eq. 1). We assume that physiologically active roots have increased exudation rate, and chose root respiration as proxy for tissue activity. Root respiration is simulated as function of root N mass and root temperature. Observations support the positive relationship between root exudation and root respiration or root N content (Akatsuki and Makita, 2020; Li et al., 2021; Sun et al., 2017, 2021). Distribution of root respiration and exudation across the vertical soil profile follows the simulated root



distribution. In addition, the slope of the linear relationship between root exudation and root respiration is assumed to be a function of nutrient status of the plant (Ataka et al., 2020; Prescott et al., 2020): C-to-nutrient ratios in the labile pool that are higher than average C-to-nutrient ratios required for tissue production will result in higher exudation (Eq. 2).

$$CEX = s * \beta_{avg} * R_{fr} \quad (1)$$

Where  $CEX$  is C root exudation in  $[gC\ m^{-2}\ s^{-1}]$ ,  $R_{fr}$  is fine root respiration in  $[gC\ m^{-2}\ s^{-1}]$ ,  $s$  [unitless] is a unitless parameter that determines maximum slope and  $\beta_{avg}$  [unitless] is the 7-days moving average of a scalar  $\beta$  reflecting nutrient shortage and surplus C in the labile pool (range 0 -1) (Thum et al., 2019), calculated by:

$$\beta = 1 - e^{-(\lambda * \Phi)^{k_{ex}}} \quad (2)$$

Where  $\lambda$  [unitless] and  $k_{ex}$  [unitless] are parameters (Table 2 for values used in this study) and the modifier  $\Phi$  represents C excess, or N and P deficiency, respectively:

$$\Phi = \Phi_C * \text{Max}(\Phi_N, \Phi_P, 1) \quad (3)$$

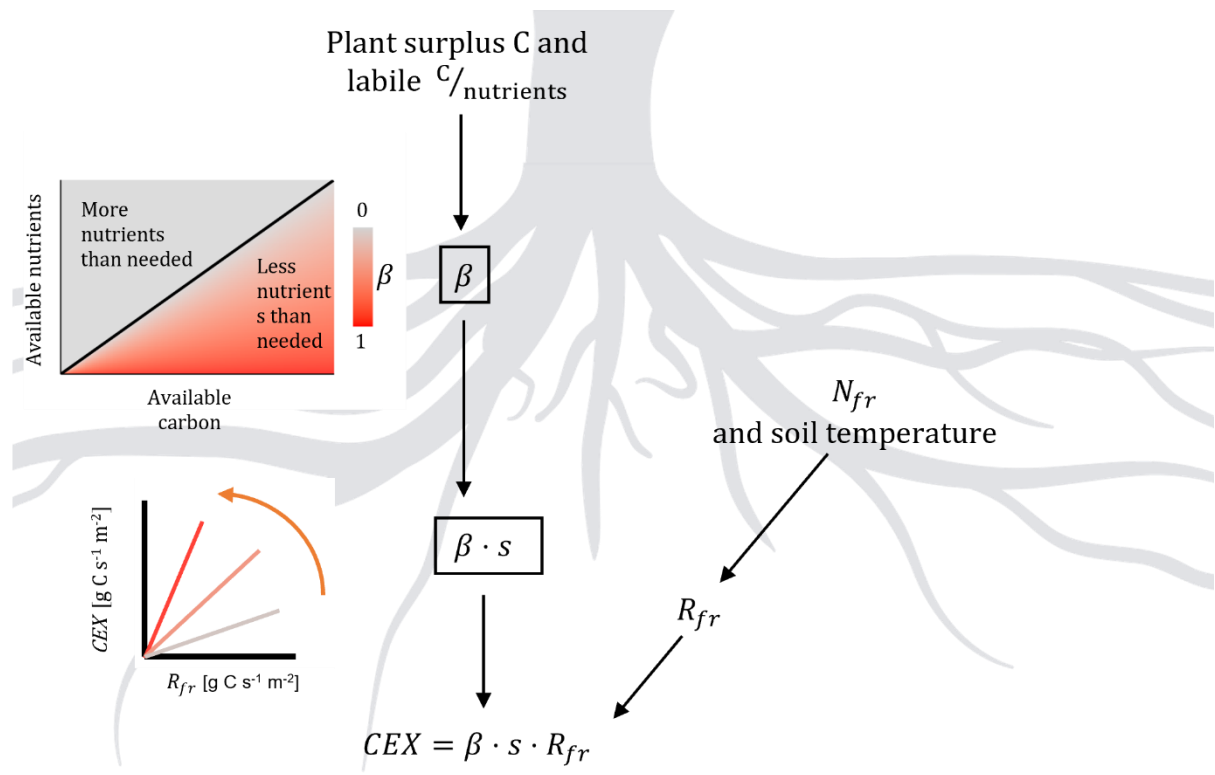
Where  $\Phi_C$  is calculated as the ratio of the actual C labile pool size ( $C_{lab}$ )  $[molC\ m^{-2}]$ , compared to the target pool size ( $C_{lab}^*$  in  $[gC\ m^{-2}]$ ).  $\Phi_N$  and  $\Phi_P$  are calculated as the ratio of labile pool stoichiometry ( $(C/N)_{lab}, (C/P)_{lab}$  [unitless]) and labile pool target stoichiometry ( $(C/N)_{lab}^*, (C/P)_{lab}^*$  [unitless]). The target labile C pool size ( $C_{lab}^*$ ) is calculated as the maximum of either the weekly sum of GPP or maintenance respiration. The N and P target labile pool sizes are calculated based on the stoichiometric last 7-day growth requirements in N and P to convert  $C_{lab}^*$  into plant biomass. The modifiers are given by:

$$\Phi_C = \text{MAX}\left(1, \frac{C_{lab}}{C_{lab}^*}\right) \quad (4)$$

$$\Phi_N = \frac{(C/N)_{lab}}{(C/N)_{lab}^*} \quad (5)$$

$$\Phi_P = \frac{(C/P)_{lab}}{(C/P)_{lab}^*} \quad (6)$$

As a result,  $\Phi$  increases under conditions in which labile C accumulates in the labile pool, and if the stoichiometry of the labile pool is wider than the target stoichiometry. The smallest value  $\Phi$  can take is 1, leading to values of  $\beta$  close to zero. We constrained  $\beta$  to values larger than 0.0125 ( $\beta_{min}$ ) reflecting a minimal root exudation flux even at saturated conditions.



260 **Figure 2: Conceptual model of the nutrient modifier for carbon root exudation (CEX). Detailed description in Eq. 1-6. CEX is calculated proportional to fine root respiration ( $R_{fr}$ ). Higher C surplus or higher C-to-nutrient ratio than needed for growth leads to increase in the modifiers. This is translated into a steeper slope for the relationship between root exudation rate and fine root respiration. Fine root respiration is calculated by fine root N content ( $N_{fr}$ ), accounting for the influence of temperature on maintenance respiration. Created with BioRender.com**

**Table 2: dynamic root exudation parameters**

Parameter	Description	Value used for this simulation	reference
$s$	Slope conversion factor/ maximum slope	4	This study
$\beta_{min}$	Minimal value for $\beta$	0.0125	This study
$k_{ex}$	Weibull parameter for beta	2	Thum et al., 2019; following sink limitation
$\lambda$	Weibull parameter for beta	0.05	This study; following sink limitation



265

## 2.4 Model application

We apply our model to the EucFACE experiment. Our goal is to quantify competing soil mechanisms on C storage for increased root exudation under eCO<sub>2</sub> in a P-limited forest. We first evaluate our model against field measurements for ambient conditions, then evaluate our results against measured CO<sub>2</sub> effects on plant C allocation to see if our model can simulate the suggested increase in root exudation under eCO<sub>2</sub>. We further quantify the simulated increase in belowground C allocation and its effect on microbial growth. To assess feedback via microbial nutrient acquisition strategies we identify sources for microbial growth in C, N and P and potential shifts in sources with elevated CO<sub>2</sub>. We conclude by comparing simulated influx and outflux of microbial necromass C, N and P pools and their turnover rates, for ambient and elevated conditions.

## 2.5 EucFACE experimental site and measurement data

The EucFACE site is located in Western Sydney, Australia (33° 37' S, 150° 44' E, 30 m in elevation) in a mature eucalypt woodland. For a detailed description of the site see (Drake et al., 2016; Ellsworth et al., 2017). The site has a subtropical transitional climate with an annual average temperature of 17 °C and mean precipitation of 800 mm yr<sup>-1</sup>. Overstorey vegetation is dominated by *Eucalyptus tereticornis*, while understorey vegetation consists of a diverse mixture of shrubs, graminoids and forbs dominated by *Microlaena stipoides* (Piñeiro et al., 2020).

The soil is characterized as aeric podosol with a loamy sand texture up to 50 cm and a sandy clay loam texture in deeper horizons. The soil has a slightly acidic pH and low fertility (Crous et al., 2015; Ross et al., 2020). Previous experiments showed that plant growth is P-limited (Crous et al., 2015). Available soil P, and plant P to soil P ratio are similar to tropical and subtropical ecosystems (Jiang et al., 2024b).

The EucFACE experiment consists of 6 FACE rings, with 25 m diameter. Three rings received ambient CO<sub>2</sub> levels and three rings were exposed to elevated CO<sub>2</sub> levels (ambient +150 ppm). In 2012 CO<sub>2</sub> was stepwise increased over a period of six months with an increase of 30 ppm every 5 weeks. In February 2013 the CO<sub>2</sub> concentration in the experiment rings reached their target of +150 ppm (Drake et al., 2016). Since then, the ecosystem has been continuously exposed to eCO<sub>2</sub>. Measurements used in this study were taken between 2013 - 2019. Major C pools, NPP and NEP under ambient conditions were measured between 2013 - 2016. A detailed description on measurement methods is provided in (Jiang et al., 2020) and (Jiang et al., 2024b). Soil respiration is taken from (Drake et al., 2018) and supplemented by additional information from (Jiang et al., 2020).

## 2.6 Model parameterization

We parameterized the model following in situ-based observations for *E. tereticornis*, taken under ambient conditions from 2013 - 2019, provided by Jiang et al., 2024 (Table A1). As no direct measurements of root exudation exist for this site, we



295 calibrated  $s$  and  $\beta_{min}$  based on the site C-budget and soil respiration data for ambient conditions from 2013-2016 (Jiang et al., 2020).

## 2.7 Model set-up and analysis

300 Simulations were done for 500 years of spin-up to reach quasi-equilibrium, with a subsequent simulation length of 325 years afterward from 1700-2024, following the modelling protocol from: (Jiang et al., 2024a): Meteorological forcing for 1700-2012 and 2019-2024 was gained from repeated and randomized observations from 2013-2018, while CO<sub>2</sub>, N and P deposition followed historic values. Forcing for spin-up repeated the first 30 years of the forcing data under 280 ppm CO<sub>2</sub>. As a result of forcing from randomized observations and meteorological extremes in observation years, and contrary to observations, our model showed a downward trend in total vegetation C from 5900 gC m<sup>-2</sup> to 5700 gC m<sup>-2</sup> between the year 2012 and 2019 (Fig. B1)

305 The mean yearly change in pools and mean yearly fluxes for simulations were calculated for 2013-2019. We calculated the effect of eCO<sub>2</sub> by subtracting results under ambient CO<sub>2</sub> conditions from result under elevated CO<sub>2</sub>. We compared the results to observed effects of eCO<sub>2</sub> on the C budget described in (Jiang et al., 2020).

We trace the fate of the additional assimilated carbon under eCO<sub>2</sub>, through the ecosystem, standardizing fluxes as the percentage of additional overstorey GPP for both simulations and observations. For aboveground fluxes, we use the overstorey aboveground biomass production, autotrophic respiration and changes in C pools. However, for belowground fluxes, i.e., heterotrophic respiration, root respiration, root biomass production and changes in soil C pools we cannot differentiate between overstorey and understorey origin. Therefore, we likely overestimate the observed change per additional overstorey GPP under eCO<sub>2</sub> in respiration fluxes.

315 For model analysis, microbial growth was calculated by the flux from the DOM to the microbes ( $F_{DOM \rightarrow MIC}^X$  [gX m<sup>-2</sup> s<sup>-1</sup>]), adjusted by the current carbon or nutrient use efficiency ( $XUE$  [unitless]) for each soil layer separately. Most measurements for soil processes at EucFACE were taken in topsoil layers, which are also typically more active. We therefore separate model outputs between topsoil (upper 50 cm) and deep soil (below 50 cm). We estimate the contribution of fluxes from root exudation, microbial recycling upon death, and decomposition of soluble litter, polymeric litter, and microbial residue to microbial growth  $F_{i \rightarrow growth}^X$  [gX m<sup>-2</sup> s<sup>-1</sup>] for topsoil by their relative production of DOM:

$$320 \quad F_{i \rightarrow growth}^X = F_{DOM \rightarrow MIC}^X * XUE * \frac{F_{i \rightarrow DOM}^X}{\sum_{i \in I} F_{i \rightarrow DOM}^X} \quad (7)$$

With  $I$  being the set of all contributing pools and  $F_{i \rightarrow DOM}^X$  [gX m<sup>-2</sup> s<sup>-1</sup>] being the according fluxes from these pools towards DOM. Similarly, we calculated heterotrophic respiration derived from the depolymerization of residue carbon  $Rh_{priming}$  [gC m<sup>-2</sup> s<sup>-1</sup>] as:

$$Rh_{priming} = F_{DOM \rightarrow MIC}^C * (1 - CUE) * \frac{F_{residue \rightarrow DOM}^X}{\sum_{i \in I} F_{i \rightarrow DOM}^C} \quad (8)$$



### 2.7.1 Turnover times

To account for adaption to sudden CO<sub>2</sub> increase, turnover times were calculated for 2015-2019. Ecosystem carbon turnover time  $\tau_{ES}$  [yr] was calculated as

$$\tau_{ES} = \frac{C_{total}}{R_{Eco}} \quad (9)$$

Where  $C_{total}$  [gX m<sup>-2</sup>]. is the combined plant and topsoil carbon and  $R_{Eco}$  [gX m<sup>-2</sup> yr<sup>-1</sup>] the ecosystem respiration. Soil turnover times  $\tau_{soil}^X$  [yr] were calculated by dividing pool sizes with their respective outgoing fluxes as

$$\tau_{soil}^C = \frac{C_{litter} + C_{soil}}{R_h} \quad (10)$$

$$\tau_{soil}^N = \frac{N_{litter} + N_{soil} + N_{inorg}}{leaching_N + U_N^{plant} + emission_N} \quad (11)$$

$$\tau_{soil}^P = \frac{P_{litter} + P_{soil} + P_{inorg}}{leaching_P + U_P^{plant} + occlusion} \quad (1213)$$

Where  $X_{litter}$  are the combined litter pools;  $X_{soil}$  are the combined organic topsoil pools and  $X_{inorg}$  as combined inorganic topsoil pools [gX m<sup>-2</sup>]. In the denominator are processes removing N or P from topsoils, e.g., heterotrophic respiration  $R_h$ , leaching, occlusion, emission and plant uptake  $U_X^{plant}$  [gX m<sup>-2</sup> yr<sup>-1</sup>].

Necromass turnover  $\tau_{necromass}^X$  [yr] time was calculated as

$$\tau_{necromass}^C = \frac{C_{necromass}}{F_{residue \rightarrow DOM}^C} \quad (14)$$

$$\tau_{necromass}^N = \frac{N_{necromass}}{F_{residue \rightarrow DOM}^N} \quad (15)$$

$$\tau_{necromass}^P = \frac{P_{necromass}}{F_{residue \rightarrow DOM}^P + Biochem_{minnecro}} \quad (16)$$

Where  $X_{necromass}$  [gX m<sup>-2</sup>] is the combined pool of microbial residues and mineral-associated microbial residues and  $Biochem_{minnecro}$  [gP m<sup>-2</sup> yr<sup>-1</sup>] is the biochemical mineralization from these pools.



### 3 Results

#### 3.1 Model evaluation

##### 3.1.1 Model performance under ambient conditions

Simulated vegetation and soil pools size and stoichiometry and vegetation fluxes under ambient conditions compared well, overall, with observations from the three control plots for the period of 2013 - 2016 (Table B1, B2). Simulated GPP had a 9 % bias, but was still within standard deviation of the observation-based estimate. There are no direct observations of root exudation at EucFACE but the model estimated mean carbon root exudation (CEX) to be  $366 \text{ gC m}^{-2} \text{ yr}^{-1}$  for ambient conditions, equivalent to 22 % of GPP. Exudation rate per gC fine root biomass amounted to  $2 \text{ gC (gC fr)}^{-1} \text{ yr}^{-1}$  and ranged from  $0.1 \text{ mgC (gC fr)}^{-1} \text{ d}^{-1}$  to  $16 \text{ mgC (gC fr)}^{-1} \text{ d}^{-1}$  on daily level, with an average C to N ratio of  $176 \text{ gC gN}^{-1}$ . Modelled soil respiration under ambient conditions is around  $1207 \text{ gC m}^{-2} \text{ yr}^{-1}$ , and thus slightly larger than the observed range of  $1097 (+86) \text{ gC m}^{-2} \text{ yr}^{-1}$ . The model estimated that soil respiration was 61% heterotrophic and 39 % autotrophic root respiration, which agree well with observations that estimated 56 % and 44 %, respectively (Jiang et al., 2020).

##### 3.1.2 Allocation patters of additionally acquired GPP

Observations indicated a major increase in belowground at the expense of aboveground biomass production. The model showed only slight changes in plant carbon allocation under  $\text{eCO}_2$  (Fig. B2) but captured the increase in belowground C allocation with a 30 % increase in CEX, compared to a 22 % increase in GPP. Additionally, the model simulates a stronger plant CUE under  $\text{eCO}_2$ , as BP increased stronger than GPP. The responses of fluxes to  $\text{CO}_2$  were considerably larger in the model than in the observations, starting with a higher GPP response (Table B3). QUINCY-JSM simulations predicted an average 22 % increase of annual GPP under elevated  $\text{CO}_2$  during 2013-2019, which represents an overestimation in comparison to the 12 % GPP stimulation shown in the observations (Jiang et al., 2020). Consequently, simulated  $\text{CO}_2$  effects on other ecosystem fluxes were higher than observations. Modelled root exudation increased 30 % (Fig. B3), and modelled biomass production increased 33 % although observations only measured a 3 % increase in BP. Both BP and CEX increase more than GPP, therefore allocation to these fluxes has increased as a result of smaller requirement for autotrophic respiration. Soil respiration increased by 13%, agreeing with the observed 12% increase, although remaining lower than the 22% increase in GPP.

Implementation of root exudation in QUINCY-JSM improved allocation of additional GPP under  $\text{eCO}_2$  but still overestimates increase in vegetation pools due to overestimation of the  $\text{CO}_2$  effect on BP (Fig. 3). Of the additional GPP under elevated  $\text{CO}_2$ , 60 % could not be measured but were assigned as root exudation (Fig. 3a,  $Ra+BP+CEX$ ). Our model estimates that vegetation allocates 30 % of additional GPP to root exudates, providing a possible explanation for the unidentified flux (Fig. 3b,  $Ra+BP+CEX$ ). Implementation of root exudation improved allocation of C towards biomass production (BP) and autotrophic respiration (Ra) compared to simulations without root exudation, as it reduced the contribution of these fluxes from 49 % to 33 % and from 51 % to 37 %, respectively (Fig. B4, Fig. B5).



In observations the increase in heterotrophic respiration corresponded to 56 % of the additional overstorey GPP (Fig. 3a, *R*). Implementation of root exudation improved the simulated contribution of heterotrophic respiration (Fig. B4, Fig. B5), but still underestimates the effect as only 28 % of additional GPP is emitted through increased heterotrophic respiration (Fig. 3b, *R*), possibly as a result of the underestimation of the effect in allocation towards root exudation.

380 Observations indicated a decrease of topsoil organic carbon equal to -12 % of the change in GPP under eCO<sub>2</sub> during the experimental phase, but the result was not significant. In our simulation eCO<sub>2</sub> led to an increase of topsoil equal to 3 % of the change in GPP. However, the model also simulates an accumulation of C in deeper soil layers equal to 7 % of the additional C uptake. Considering the strong variation in measurements regarding soil organic C (SOC) pools we assume that our simulations are in agreement with observations regarding topsoil C pools.

385

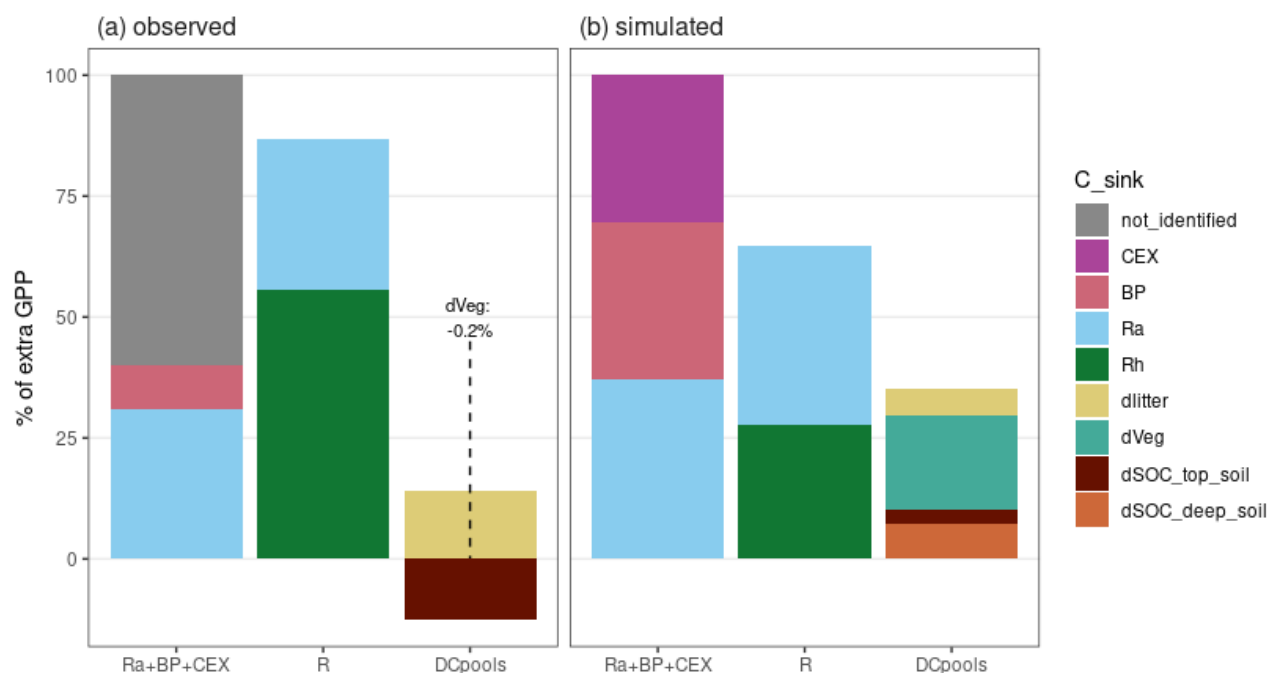


**Figure 3: Comparison of the fate of additional sequestered C under CO<sub>2</sub> as percentage of increased overstorey gross primary productivity (GPP) for a) observations (2013-2016) (Jiang et al., 2020) and b) simulations (2013-2019).** For simulations additional GPP is transferred into autotrophic respiration (*Ra*), biomass production (*BP*) and root exudation (*CEX*). For observations *CEX* was not measured. Ecosystem respiration (*R*) is composed of heterotrophic respiration *Rh* and autotrophic respiration *Ra*. Change in ecosystem carbon pools is composed of change in topsoil organic C (*dSOC\_top\_soil* top 10 cm for observation, top 50 cm for simulation), change in deep soil SOC (*dSOC\_deep\_soil*, no observations) change in litter (*dlitter*) and change in vegetation (*dVeg*).

390





## 3.2 Simulated effects of eCO<sub>2</sub> on soil biogeochemistry

### 3.2.1 Microbial growth dynamics

395 In the model, eCO<sub>2</sub> increased belowground input disproportionally through high root exudation. However more than half of these got directly respired, increasing the fraction of heterotrophic respiration originating from root exudation. Microbial growth increased by 14 % in topsoil layers but increased accumulation of C in soil pools is mostly caused by sequestration in deeper soil layers, with less microbial activity (Fig. 4). In the simulation, eCO<sub>2</sub> led to an increase in both biomass production and root exudation, resulting in an increase in soil C input of 158 gC m<sup>-2</sup> yr<sup>-1</sup>. This equals an increase of 20 % compared to  
400 ambient conditions. While input under ambient treatment was composed of 45 % root exudation, the additional input under eCO<sub>2</sub> was composed of 70 % root exudation and to 30 % litter (Fig. 4, *soil C input*). At the same time, eCO<sub>2</sub> increased heterotrophic respiration by 101 gC m<sup>-2</sup> yr<sup>-1</sup>. Under ambient conditions 92 % of C input was respired. Due to change of input composition and input into deeper soil layers through root exudation, only 64 % of the additional C input into the soil system was emitted as additional heterotrophic respiration. We partitioned the additional heterotrophic respiration under eCO<sub>2</sub> into  
405 three components. More than 50 % of the additional heterotrophic respiration originated from respiration of root exudates (Rh\_CEX), 15 % from depolymerisation of microbial necromass (Rh\_res), i.e., microbial residues (+ 9 % increase compared to ambient conditions), and the rest from respiration of recycled microbial biomass, soluble and polymeric litter and degradation of woody biomass (Rh\_other). The direct loss of more than 50 % of additional root exudation suggests that in the model root exudates in topsoil layers are directly consumed by microbes, and then respired according to the assumptions for  
410 microbial carbon-use efficiency, that is dependent on the stoichiometric imbalance of between the source material and microbial biomass, and constrained within a range of 30% to 50%.

Increased input of C increased microbial growth by 53 gC m<sup>-2</sup> yr<sup>-1</sup>, which is equivalent to 34 % of the additional C input, and represents a 14 % increase over ambient conditions (Fig. 4, *microbial growth*). Although the increase in microbial growth was most prevalent in topsoil, it was not accompanied by an increase in soil organic C. Instead, eCO<sub>2</sub> led only to an increase in 10  
415 gC m<sup>-2</sup> yr<sup>-1</sup> in topsoil C, equivalent to 6 % of the additional C input, indicating that microbial increased decomposition for nutrient acquisition offset necromass build up. As root exudation followed root distribution, increased root exudation resulted in increased C input into deeper soil layer. Therefore additional 26 gC m<sup>-2</sup> yr<sup>-1</sup> accumulated in deeper soil layers. However, small microbial growth suggests that the underlying mechanism is the sorption of additional DOC input to mineral surfaces. As microbes did not decompose most of additional litter input over the experimental phase, eCO<sub>2</sub> resulted in an increase of 20  
420 gC m<sup>-2</sup> yr<sup>-1</sup> in litter pools (Fig. 4, *change in C pools*). The results indicate that root exudates and depolymerization of necromass are valuable sources for microbial growth under eCO<sub>2</sub>.

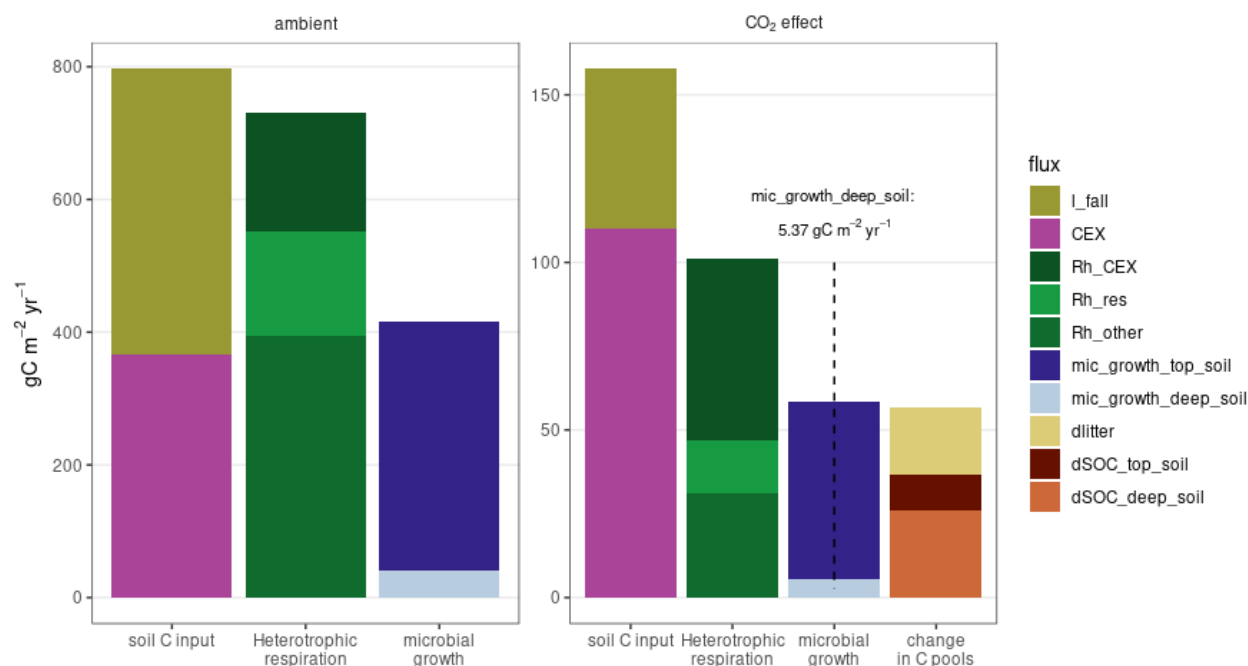


**Figure 4: simulated sources and sinks for C in soil at EucFACE under ambient conditions and as CO<sub>2</sub> effect, displayed as yearly average for 2013-2019. Additional C input is composed of litterfall (*l\_fall*) and exudation (CEX). Elevated CO<sub>2</sub> induced increased heterotrophic respiration (Rh), which originated from respiration of exudation (Rh\_CEX), respiration of microbial residues (Rh\_res) and respiration of degradation of woody biomass and respiration of directly recycled microbial biomass, soluble and polymeric litter (Rh\_other). Additionally, eCO<sub>2</sub> affects microbial C growth in top (*mic\_growth\_top\_soil*) and deep soil (*mic\_growth\_deep\_soil*), change in litterpools (*dlitter*), topsoil (50 cm) organic C (*dSOC\_top\_soil*) and deep soil organic C (*dSOC\_deep\_soil*).**

### 3.2.2 Microbial resource acquisition

In the model, increased root exudation induced by eCO<sub>2</sub> increased microbial growth and biomass. Nutrients required for microbial growth were mostly gained from organic sources. Increased root exudation supplied the majority of the additional microbial growth in C, namely 60 %. To the contrary root exudation only contributed 2 % of N to additional microbial growth (Fig. 5 a, b), caused by low C: N ratio of root exudation. Instead, microbes obtained additional N for growth via uptake of soluble inorganic nitrogen (24 % of additional growth) and asymbiotic N fixation (2 % of additional growth), recycling upon microbial death (32 % of additional growth) and microbial residue depolymerization (36 % of additional growth). As a consequence, organic sources, rather than inorganic sources, supplied additional growth in N, showing that increased C input under eCO<sub>2</sub> also increased necromass decomposition. The increased microbial uptake of inorganic N led to a net N mineralization decrease by 14 % (Fig. B6). For P, inorganic soluble P uptake supplied most of the P for additional microbial growth under eCO<sub>2</sub>, namely 58 %. This also included PO<sub>4</sub> that was mobilized by biomineralization. Only 42 % of P for



additional microbial growth originate from uptake of DOP, mostly from microbial recycling which contributes 36 % (Fig. 5 c).

We further investigated the effect of  $e\text{CO}_2$  on percentage contribution of sources for microbial growth in C, N and P, respectively. For C, the contribution of root exudation increased from 30% to 34 %, while for N and P contribution of nutrient sources remains relatively constant and depended on organic sources (Fig. 5 d-f). nitrogen was to 77 % (elevated: 75 %) derived from organic sources, such as microbial recycling and depolymerized microbial necromass (Fig. 5 e). For P, 45 % (elevated: 46 %) of microbial growth came from uptake of soluble phosphate (Fig. 5f). Contribution of nutrient sources remain nearly constant, because of model assumptions and simulated nutrient conditions. Recycling of microbial biomass is based on a fixed parameter; therefore, we expect little change regarding this flux. For N,  $\text{NH}_4$  availability and flexibility in asymbiotic N fixation were sufficient to supply inorganic sources preventing an increase in contribution from decomposition. Similar to N, recycling of microbial P follows a fixed parameter. Uptake through decomposition of microbial residue is mostly determined by microbial N and C limitation and P input through litter under  $e\text{CO}_2$  is negligible. However inorganic P uptake includes phosphate from available sources and phosphate released through biomineralization. We therefore investigated P dynamics in greater detail.

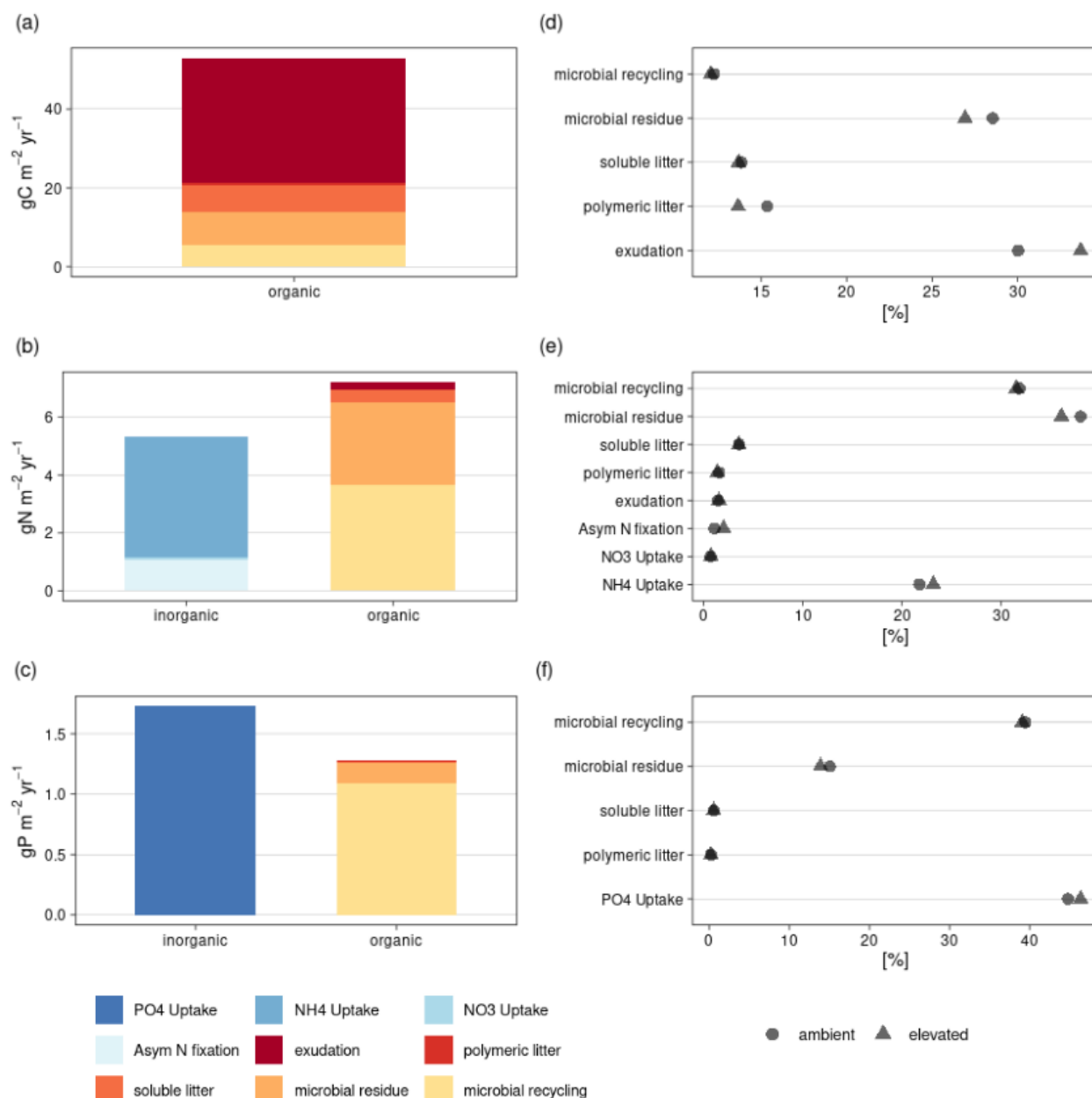


**Figure 5: Simulated uptake sources (C, N, P) for microbial growth at EucFACE in topsoil (50 cm), averaged for 2013-2019, calculated based on contribution of sources to DOM and microbial CUE. (a-c)  $\text{CO}_2$  effect on sources of uptake of C, N and P, respectively; (d-f) distribution of nutrient sources for microbial growth under ambient and elevated conditions. In (e-f) sources are divided into organic and inorganic (N and P only). Organic sources are exudation, uptake from depolymerised microbial residue, uptake from directly recycled microbial biomass and litter. Sources for inorganic N uptake are soluble  $\text{NH}_4$  and  $\text{NO}_3$  and asymbiotic N fixation of  $\text{N}_2$ . Inorganic P uptake is uptake of  $\text{PO}_4$ . However, a significant amount of this  $\text{PO}_4$  is gained by biochemical mineralization of organic material (Fig. 6).**



Increased microbial uptake of  $\text{PO}_4$  under  $\text{eCO}_2$  was primarily driven by solubilization of  $\text{PO}_4$  through biochemical mineralization (Fig. 6). Biochemical mineralization of organic matter increased by 22 % ( $1.5 \text{ gP m}^{-2} \text{ yr}^{-1}$ ) in comparison with ambient conditions (Fig. B6). Elevated  $\text{CO}_2$  affected biochemical mineralization more than gross biological mineralization or weathering, which increased by 11 % ( $0.3 \text{ gP m}^{-2} \text{ yr}^{-1}$ ) and 7 % ( $<0.01 \text{ gP m}^{-2} \text{ yr}^{-1}$ ) respectively. Increased microbial uptake matched increased gross biological and biochemical mineralization, thereby confirming that microbes derived additional P from organic sources (Fig. 6a). Although  $\text{eCO}_2$  resulted in an overall 40 % increase in net  $\text{PO}_4$  mineralization, the effect was variable over the experimental period (Fig. 6 b). Nonetheless the simulation resulted in an increase in available inorganic  $\text{PO}_4$  (Fig. B7).

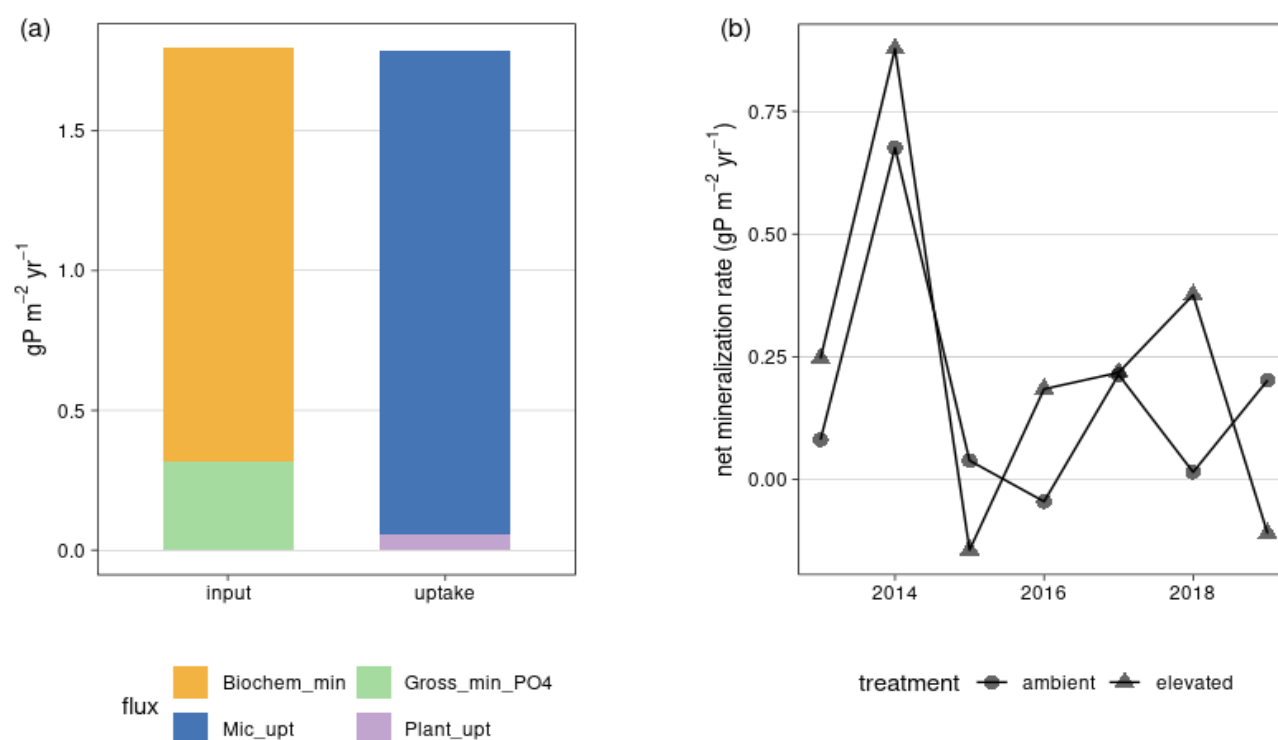


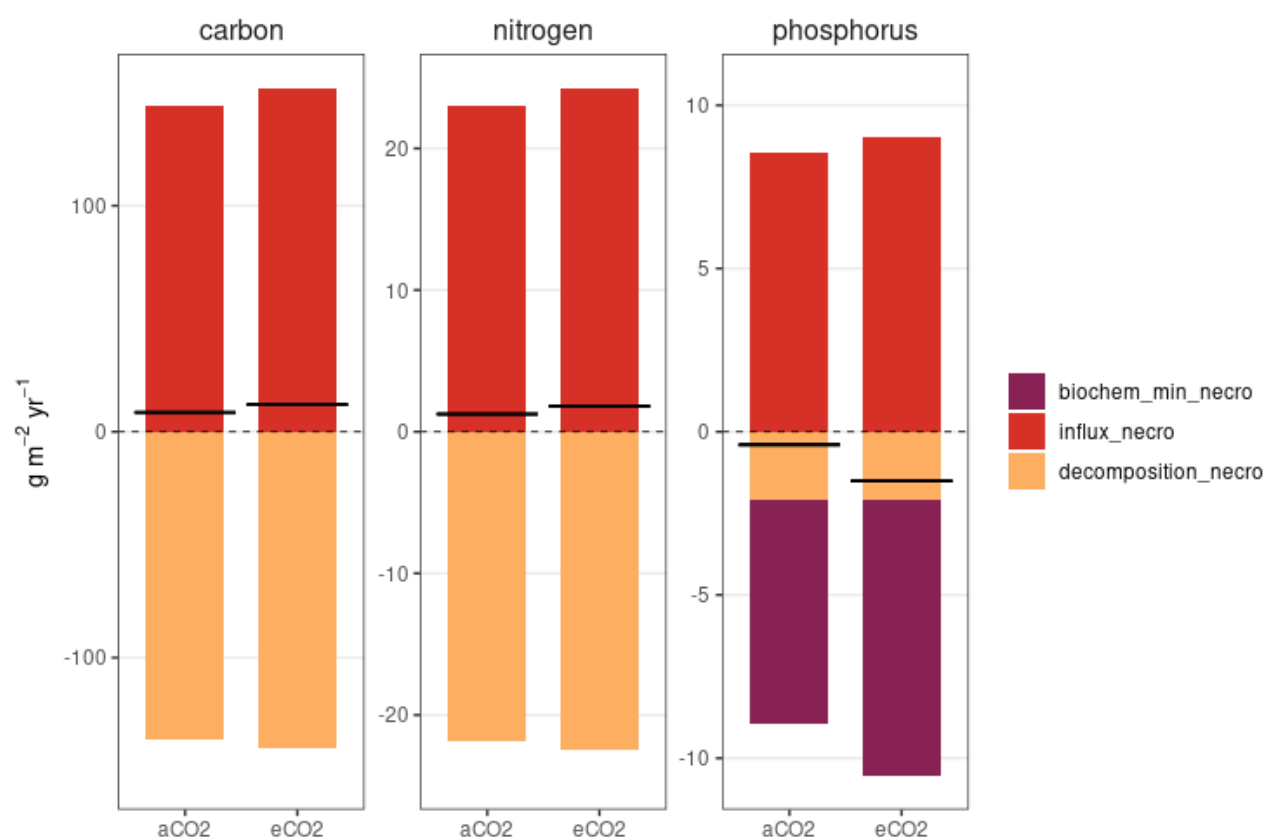
**Figure 6: simulated  $\text{CO}_2$  effect on mineral P fluxes in topsoil layers (50cm).** (a) Yearly average from 2013-2019 fluxes which provide (input) plant and microbes available mineral P are gross biological mineralization and biochemical mineralization. Available P get immobilized via uptake by microbes or plants. Adsorption and weathering are not displayed as the  $\text{CO}_2$  effect on these fluxes is below  $0.01 \text{ gP m}^{-2} \text{ yr}^{-1}$  (b) net  $\text{PO}_4$  mineralization simulated for 2013-2019 for ambient and elevated  $\text{CO}_2$

### 3.2.3 Cycling of microbial necromass

Microbial growth and nutrient acquisition under  $\text{CO}_2$  increased tops-soil microbial necromass build-up and decomposition, therefore accelerating the cycling of SOM. We separated top-soil microbial necromass growth into input and output fluxes for topsoil (Fig. 7). The  $\text{CO}_2$ -induced increase in microbial growth led to a 13 % increased input flux towards microbial necromass (microbial residue and the organo-mineral associated microbial residues) for C, N and P compared to ambient conditions (Fig.



7). However, increased depolymerization under eCO<sub>2</sub>, as result of increased priming activity and biochemical mineralization also led to increased outgoing fluxes (C: 8 %, N: 8 %, P: 30 %). Under ambient CO<sub>2</sub>, the net balance in microbial C, N  
485 necromass cycling was close to zero. The net effect of CO<sub>2</sub> on the microbial necromass (including organo-associated) cycling was small for all elements relative to the size of in- and outgoing fluxes and to the pools themselves. For C and N, the effect of eCO<sub>2</sub> was positive leading to a 11 gC m<sup>-2</sup> yr<sup>-1</sup> and 2 gN m<sup>-2</sup> yr<sup>-1</sup> increased net input through microbial necromass compared to ambient conditions. For microbial necromass P, increased biochemical mineralization led to a negative net effect in P necromass cycling of - 3 gP m<sup>-2</sup> yr<sup>-1</sup>. Both, increased depolymerization and increase biochemical mineralization were driven  
490 by increased microbial biomass and changes in enzyme allocation (Fig. B8, Fig. B9) Despite this net effect, the overall necromass P pool changed by only 2 %. We also found that, P remained in the ecosystem and was transferred to faster cycling pools, namely microbial biomass or dissolved organic matter (Fig. B10, Fig. B11). Consequently, increased root exudation left the quantity of topsoil SOM nearly unchanged, but increased its turnover rate



495 **Figure 7: Simulated balance of C, N and P for microbial necromass (combined pool of microbial residues and mineral associated microbial residues) in topsoil (50 cm) under ambient and elevated CO<sub>2</sub>. Influxes (red, above the dashed line) are compared with outfluxes (yellow, below the dashed line) and, for P, biochemical mineralization (purple, below the dashed line). Black lines represent the net effect.**



500 Elevated CO<sub>2</sub> led to an acceleration of biogeochemical cycling in the ecosystem (Table 3). Ecosystem carbon turnover time decreased by 10 %, caused by faster respiration of soil inputs. In soils elevated CO<sub>2</sub> had a more pronounced effect on P (20 % decrease) and N (20 % decrease), then on carbon cycling (12 % decrease), possibly caused by increased plant nutrient uptake to sustain BP. As, in the model, C and N cycling of microbial necromass are closely interlinked, turnover times of microbial necromass decreased by 9 % for C and N. For P enhanced biochemical mineralization caused a further decrease in necromass turnover time by 21 %.

505

**Table 3: Modelled turnover times under ambient and elevated CO<sub>2</sub> for the ecosystem (C), soil (C, N, P) and microbial necromass (C, N, P). Calculated for 2015-2019.**

		$\tau_{ES}(yr)$	$\tau_{soil}(yr)$	$\tau_{necromass}(yr)$
carbon	aCO <sub>2</sub>	10.2	17.1	30.4
	eCO <sub>2</sub>	9.2	15.1	27.7
nitrogen	aCO <sub>2</sub>	-	242.1	30.5
	eCO <sub>2</sub>	-	193.2	27.7
phosphorus	aCO <sub>2</sub>	-	561.2	8.2
	eCO <sub>2</sub>	-	447.6	6.4



## 510 4 Discussion

We developed and tested a model implementation for dynamic root exudation in a microbial explicit terrestrial biosphere model and analyzed the consequences for increased root exudation under eCO<sub>2</sub> in a mature Eucalyptus forest. We found that – in our model – increased root exudation represents a possible explanation for not measured GPP allocation fluxes under eCO<sub>2</sub>. We analyzed how much of additional C input under eCO<sub>2</sub> was matched by increased heterotrophic respiration and how  
515 microbial nutrient acquisition contributed to further heterotrophic respiration and SOM cycling. Our simulations show that more than 60 % of additional C input into soils was matched with increased heterotrophic respiration for of two main reasons. First, microbes respired a substantial amount of the new C input, primarily root exudation. Second, enhanced necromass decomposition for nutrient acquisition offset increased necromass input, both driven by microbial growth. As a result, our model simulated only minor increases in topsoil C under eCO<sub>2</sub>. The implementation of root exudation, provided a reasonable  
520 explanation for the partitioning of additional GPP and is in better agreement with observations. We discuss our results by focusing on the effect of eCO<sub>2</sub> on plant carbon allocation, heterotrophic respiration, microbial growth and microbial necromass cycling in the context of plant-microbe interactions. Where possible we evaluate our results against previous studies and discuss model assumptions in relation to discrepancies.

### 4.1 Plant carbon allocation and root exudation

525 Observations in allocation of plant surplus GPP suggest a major C allocation belowground, suggested by increased soil respiration under eCO<sub>2</sub>. Our model agrees with the increased belowground allocation under eCO<sub>2</sub> as a 22% increase in GPP, led to a 30 % increase in root exudation. Implementation of root exudation into the model also improved allocation of surplus GPP. However, even with root exudation, the model continued to overestimate the response in autotrophic respiration and BP, compared to observations. It is likely that our model does not yet replicate the full complexity of P limitation under eCO<sub>2</sub> on  
530 the system (Crous et al., 2015), therefore still allocating more C towards biomass production and less to soils than measured. Plant P availability under eCO<sub>2</sub> may be caused by the overestimation of organic soil pools, caused by strong accumulation in organic mineral-associated pools. These pools do not directly determine C and N availability but are a P source through biochemical mineralization. Additionally, our model may underestimate the strong competition for PO<sub>4</sub> by microbes and sorption to soil, suggested by the P budget of the site (Jiang et al., 2024b).

535 It is unlikely that we underestimated the ambient root exudation flux, since the simulated ratio of root exudation to GPP under ambient conditions of 21 % is already very high compared to global estimations: For example, Chari et al. (2024) suggest that across 6 different biomes globally 5.6 % of GPP is allocated to root exudates, but with strong variations between biomes and measurements. On the other hand, plant growth in EucFACE is P-limited which could explain higher exudation rates. Nevertheless, it is possible that the simulated effect of eCO<sub>2</sub> on root exudation is too small. In the model, eCO<sub>2</sub> enhanced  
540 yearly root exudation rate per area and per fine root mass of up to 30 % during 7 years of CO<sub>2</sub> increase. Even though, the compiled carbon budget suggests an increased C allocation belowground (Jiang et al., 2020), a direct evaluation of the eCO<sub>2</sub>





effect is impossible because there are no direct measurements of root exudation and large uncertainties are associated with the other components of the ecosystem carbon budget. In the Duke FACE experiment,  $e\text{CO}_2$  was estimated to cause a 40 % increase in allocation to exudates and fungi (Drake et al., 2011) and in BIFoR FACE root exudation was estimated to increase by 42-63 % (Norby et al., 2024), but these effects were statistically not significant. In our simulation the increase in root exudation emerges from plant nutrient, C surplus status and fine root growth. A stronger P limitation of plant growth under  $e\text{CO}_2$  may increase the  $\text{CO}_2$  effect on root exudation and reduce allocation to BP in the model.

## 4.2 Heterotrophic respiration

Additional allocation of C to soil is potentially offset by additional heterotrophic respiration caused by two mechanisms: direct respiration of fresh material and respiration of old material, i.e., priming. Our model suggests that both mechanisms contribute to increased heterotrophic respiration under  $e\text{CO}_2$ , with direct respiration having a stronger impact. Root exudation was the major additional soil C input under  $e\text{CO}_2$ , but microbes directly respired more than half of the additional root exudation. Therefore,  $e\text{CO}_2$  only increased microbial growth by 14 %. The increased growth caused priming effects, i.e., decomposition of microbial necromass, and resulted in a further increase in heterotrophic respiration.

There is no analysis on the origin of increased heterotrophic respiration in EucFACE, but our results are consistent with other studies showing that under  $e\text{CO}_2$  the majority soil respired C originates from new soil C input (van Groenigen et al., 2017; Taneva et al., 2006). The fraction of C that is respired from microbial DOM uptake is determined by microbial carbon use efficiency. Our model showed a yearly average microbial CUE between 40 % and 50 %, which did not change under  $e\text{CO}_2$  (Fig. B12). A reduced microbial CUE under additional carbon input would lead to less microbial growth and an even larger proportion of root exudation as the source for heterotrophic respiration. Taking into account the important role of microbial growth and necromass for SOM formation (Miltner et al., 2012), the rapid respiration of fresh material and the additional decomposition of old material questions the capability of soils to sequester large amounts of C under  $e\text{CO}_2$  in this system.

## 4.3 Microbial growth and nutrient feedback

Our model suggests a coupling of processes such that larger root exudation flux increased microbial growth, which increased depolymerisation for N acquisition and biochemical mineralization for P acquisition. Enhanced biochemical mineralization increased  $\text{PO}_4$  availability. In the model, root exudation disproportionally drove microbial growth in C under  $e\text{CO}_2$ , suggesting that microbes might change their diet under  $e\text{CO}_2$  to more easily available and more easily degradable substrates to gain carbon (Ai et al., 2023; Dijkstra et al., 2013; Zhou et al., 2021). Simulated root exudation showed a C to N ratio of 176 and contained no P, whereas microbial C to N ratio was 4.3 (N: P = 4.1). Consequently, increased root exudation enhanced microbial demand for nutrients. For N, this demand was partially satisfied by available inorganic N. As a result, microbial nutrient uptake from organic sources increased, but without a substantial shift in the contribution. Here our model partially disagreed with field observations: Measurements of soil enzymes found no increase in N-degrading enzymes or microbial nutrient limitations under



eCO<sub>2</sub> (Pihlblad et al., 2023). However, it is questionable if this effect would be statistically detectable in a FACE experiment, with inherently low sample size and difficulties in detecting changes in the soil (Filion et al., 2000).

575 In our model, increased biochemical mineralization satisfied additional microbial P demand. Therefore, organic sources substantially supported microbial growth in P. Microbes took up more than 95 % of the additional mineralized PO<sub>4</sub>. Even though this underlines the microbial competitiveness for PO<sub>4</sub> at this site, the positive effect of additional gross mineralization to plant PO<sub>4</sub> availability may still be overestimated (Jiang et al., 2024b). Consequently, elevated CO<sub>2</sub> led to an increase in available PO<sub>4</sub> of 20 %. This is partially consistent with observations which report increased PO<sub>4</sub> concentrations under eCO<sub>2</sub> in  
580 the rhizosphere or deeper soil layers (Hasegawa et al., 2016; Ochoa-Hueso et al., 2017; Pihlblad et al., 2023). To our knowledge it is not yet resolved which processes caused the increased PO<sub>4</sub> concentration in EucFACE. Observations from other ecosystems report increased phosphatase activity under P limitation (Marklein and Houlton, 2012) and in ecosystems with high soil organic P content (Margalef et al., 2017). In EucFACE, eCO<sub>2</sub> caused no significant increase in phosphatase at the start of the experiment (Hasegawa et al., 2016), after 1 1/2 year (Ochoa-Hueso et al., 2017) or after 4 1/2 years (Pihlblad et al.,  
585 2023).

An alternative pathway may be increased exudation of carboxylates, which could have increased PO<sub>4</sub> concentrations via ligand exchange with Fe-Al-oxides at soil surfaces (Hinsinger, 2001; Wang and Lambers, 2020). Increased carboxylate exudation has been reported for common EucFACE understorey species (Hasegawa et al., 2023). As we do not consider these processes in our model, the model resolves enhanced P requirements with increased biochemical mineralization, triggered by increased  
590 microbial growth but also by increased enzyme allocation. For N and P old SOM, e.g., necromass, therefore remained an important part for microbial nutrient supply under eCO<sub>2</sub>.

#### 4.4 Necromass cycling

Our model supports the theory that eCO<sub>2</sub> can lead to increased cycling of SOM without substantial increases in pool size (Drake et al., 2011; van Groenigen et al., 2014; Kuzyakov et al., 2019). While observations found no increase in topsoil C, our  
595 simulation led only to a minimal increase in soil organic C in topsoil layers. Our results suggests that for microbial necromass, an essential part in C storage, increased input through microbial growth and increased decomposition for microbial nutrient acquisition counteract each other. There are no continuous measurements from EucFACE analyzing changes in age composition of soil organic matter. However, using a combination of litter bag and isotopic signature measuring, Castañeda-Gómez et al. (2020) showed that eCO<sub>2</sub> led to stronger losses of old SOC and increased input of new SOC at EucFACE in  
600 summer months.

Along with C, eCO<sub>2</sub> also increased N and P turnover in our simulations. For P, also pool sizes have changes such that P is mostly transferred from slow cycling microbial necromass to fast cycling microbial biomass. This disagrees with a recent study analyzing the P budget for EucFACE, concluding that eCO<sub>2</sub> treatment led to no significant changes of soil organic P pools (Jiang et al., 2024b). However, the simulated changes were small (e.g. < 2 % in necromass) and therefore it is questionable if  
605 they could have been detected in field observations.



Uncertainties in effects on necromass cycling arise from other processes we did not consider in our model, such as flexible recycling of N under eCO<sub>2</sub>, or higher N content of root exudates, that might prevent priming effects. Additionally, in our model, eCO<sub>2</sub> caused a desorption in mineral-associated necromass. This led to more microbial-available N-rich material and may have enhanced the CO<sub>2</sub> effect on SOM decomposition.

#### 610 4.5 Comparison to other models

Implementing root exudation in QUINCY-JSM did improve the predicted CO<sub>2</sub> response of C allocation, but results still indicate that further development is necessary. A recent model inter-comparison study demonstrated that most C-N-P cycle models, including QUINCY-JSM, overestimate the C sequestration of the EucFACE ecosystem under eCO<sub>2</sub> (Jiang et al., 2024a). In contrast to observations, the majority of models simulated a positive effect on net ecosystem productivity (NEP) 615 under eCO<sub>2</sub>. Additionally, all, except one model in (Jiang et al., 2024a), allocated most additional C fixed under eCO<sub>2</sub> to either autotrophic respiration, storage or structural biomass, and underestimated the increase in soil heterotrophic respiration. The exception was GDAYP, which implemented root exudation but no microbial dynamics and therefore simulated higher soil P immobilization under eCO<sub>2</sub>.

Implementing root exudation improved the allocation of additional GPP: Compared to other models in Jiang et al. (2024a) and 620 QUINCY-JSM without root exudation, and consistent with observations, in QUINCY-JSM with root exudation reproduces the increase in C respired via heterotrophic respiration and the decrease in C lost through autotrophic respiration. Additionally, less C remains in the system in form of increased vegetation pools (Fig. B4). Consequently, the implementation of root exudation does improve the simulated CO<sub>2</sub> effect on heterotrophic respiration. However, adding root exudation flux to QUINCY-JSM did not improve the NEP response to eCO<sub>2</sub>. The response is still stronger than observed, caused by 625 accumulation of C in vegetation biomass and deep soil layers. While the first one is caused by an overestimation of BP, the latter is caused by the allocation of root exudation in deeper soil layers, as - in our model - root exudation followed root distribution, causing increased C input in layers with low microbial activity. Regardless of root exudation, QUINCY-JSM is consistent with observations in simulating weak response of topsoil C to eCO<sub>2</sub> (Fig. B11). However, in the version without root exudation this is caused by low C soil input in form of litter, rather than by fast respiration of root exudates and priming 630 effects. The current version of QUINCY-JSM simulates an increase in net P mineralization under eCO<sub>2</sub>, regardless of the implementation of root exudation. Therefore, it remains difficult to evaluate the actual effect of the implementation on PO<sub>4</sub> mineralization. Further model adjustment is needed to fully understand the feedback of plant-microbe interactions on plant nutrient uptake under eCO<sub>2</sub>.

#### 4.6 Suggestions for further advancements in modelling and experimental work

635 In the following we discuss modelling advancements and experimental work that could help to optimize representation of plant-soil interactions. We assess factors influencing plant nutrient availability and plant carbon allocation. We further provide



methodological directions for upcoming FACE experiments that would advance understanding of root exudation and microbial representation and their implementation in models under eCO<sub>2</sub>.

#### 4.6.1 Soil Phosphorus availability

640 FACE experiments suggest a strong interaction between nutrient limitation and CO<sub>2</sub> fertilization effect, but it remains uncertain how effectively current models represent nutrient limitation (Jiang et al., 2024b; Zaehle et al., 2014). The simulated, but not observed, response of BP, suggest that we underestimate the P limitation on plant growth under eCO<sub>2</sub> in our model. Overestimation in P pools may be solved with alternative model initialization approaches. However, PO<sub>4</sub> plant availability also depends on chemical and biochemical mechanisms like sorption, biochemical mineralization, and plant-microbe-  
645 competition.

For validation with field conditions, Hedley fractions can be used to determine of extractability of P in soils, which can be translated in pools used in models (Hedley et al., 1982; Helfenstein et al., 2024). We further suggest future model development should consider the improved representation of sorption dynamics (Yu et al., 2023) and the influence of site-specific soil properties namely pH or Fe-Al-oxides on them (Wang et al., 2022). Aspects like C or N cost for biochemical mineralization,  
650 accessibility of mineral-associated material for phosphatase or plant competitiveness against microbes need further investigation but currently lack data for parameterization.

#### 4.6.2 Priming effects and soil organic matter decomposition

Our model emphasizes the role of old organic matter as nutrient source, but the discrepancies need to be further explored in models and field experiments. In comparison to most other models, which directly prescribed priming (Jiang et al., 2019; Thurner et al., 2024), our study provides an advancement by representing priming effects as an emergent process mediated by  
655 microbes. We found the priming effect was small because nitrogen acquisition via other sources was possible. Nonetheless priming effects may play a more prominent role in N-limited systems as increased degradation of necromass has the potential to reduce long-term carbon sequestration. However, the majority of ecosystem models currently lack representation of this process (Jiang et al., 2024a; Walker et al., 2015).

660 Key aspects for further research include the influence of different soil properties, such as pH and soil nutrient status, on priming (Bastida et al., 2019; Spohn et al., 2013; Sun et al., 2019) and feedback of SOM decomposition on plant nutrient availability. It is also uncertain to what extend eCO<sub>2</sub> causes desorption of necromass, which may contribute to priming by increasing the material available for decomposition. In field experiments, artificial root exudates can be used to simulate the effect of additional input of labile C into soils and produce evaluation output for models (Lopez-Sangil et al., 2017).



#### 665 4.6.3 Modelling dynamic root exudation

Global mean rates of root exudation can be benchmarked against with broad meta-analysis such as Chari et al. (2024). However, additional research is needed to understand the variation of root exudation with plant species and ecosystem properties to improve model representation (Brunn et al., 2022; Chari et al., 2024; Hasegawa et al., 2023). For example, research is needed to identify patterns of root exudation in the context of atmospheric CO<sub>2</sub> increase on ecosystem level: Direct  
670 measurements used for example in BiforFACE or DukeFace (Drake et al., 2011; Norby et al., 2024) provide reliable data for model evaluation. Such measurements should consider scaling into ecosystem level e.g. (units of mass/surface area/time), implying a scaling by other observables such as root mass or soil volume (Norby et al., 2024), and seasonal changes of root exudation (Leuschner et al., 2022; Phillips et al., 2008; Zhang et al., 2022). Additionally, nutrient fertilization experiments (Ataka et al., 2020) or measurements along nutrient gradients (Jiang et al., 2022; Meier et al., 2020) help to unravel the  
675 relationship of plant nutrient, C surplus status and root exudation, and therefore to constrain model parameters.

A key limitation of our model is the lack of consideration of the chemical composition of root exudates: Next to being a source for C and nutrients for microbes, the composition of exudates can actively shape the microbial community, affect soil pH, suppress sorption of inorganic P from mineral surfaces (Jones et al., 2004). Our analysis suggests that the pure implementation of root exudation as substrate for microbial growth does not capture all of the observed P dynamics.

#### 680 4.6.4 Representation of soil microbial organisms

Uncertainty also arises from parameterization and representation of microbial pools. Currently only a few ecosystem models implement microbes explicitly (QUINCY-JSM (Yu et al., 2020); OCHDX (Zhang et al., 2020); CLM5-MIMICS-CN (Wieder et al., 2015)). In these models, carbon-use-efficiency is a key parameter as it determines how much C initially enters the microbial cycle. In QUINCY-JSM, carbon-use-efficiency is dynamically determined by the microbial nutrient imbalance, to  
685 represent microbial community changes. Other modelling approaches make use of explicitly representing distinct decomposer pools with different stoichiometric requirements, to account for changes in turnover or stoichiometry (Zhang et al., 2020). Increased inputs of root exudation with high C-to-nutrient ratio under eCO<sub>2</sub> will increase mining of nutrients by bacterial communities (Chertov et al., 2022) or benefit fungal communities (Sistla et al., 2014). Further field studies are required to evaluate whether this affects soil C storage and respiration by measuring changes in microbial biomass, stoichiometry and  
690 community composition.

## 5. Conclusion

In this study we tested a novel mechanism of dynamic root exudation in a nutrient enabled terrestrial biosphere model, and demonstrated improved the representation of the CO<sub>2</sub> effect on plant C allocation as observed in a mature forest FACE experiment Our model exemplifies, how root exudation, as the hidden pathway of plant-soil carbon cycle, can contribute to  
695 offset increases in GPP under eCO<sub>2</sub> due to increased heterotrophic respiration caused by direct respiration of exudates and



increased decomposition of microbial necromass. We suspect that increased root exudation under eCO<sub>2</sub> may lead to increased soil respiration in many nutrient-limited ecosystems worldwide, altering the soil carbon cycle through priming of microbial necromass and increased cycling of soil organic matter. We therefore recommend further development in explicit representation of root exudation, microbial dynamics and plant-microbe-interactions to account for these effects in global models.

700



**5 Appendix A: Changes in parameters and processes compared to standard QUINCY-JSM**

To improve simulations under ambient conditions, we calibrated several parameters in QUINCY-JSM for simulations of EucFACE (Table A1). Additionally, we changed processes in microbial decay to allow for priming effects in QUINCY-JSM and altered inorganic soil P initialization for deeper soil layers to account for highly weathered soils in EucFACE. To account for low P levels in subsoils of deeply layered soils, we decline simulate an exponential decline in initial inorganic P pools (assoc\_slow, occluded, primary, solute and assoc\_fast) below 70cm depth.

**5.1 Calibrated Parameters**

**Table A 1: Parameters changed in QUINCY-JSM for EucFACE simulation**

parameter	description	unit	QUINCY-JSM standard	This study	reference/reason for change
soil					
microbial_cue_max	Maximal microbial carbon use efficiency	[unitless]	0.6	0.5	Adjust to meet microbial biomass in EucFACE
k_slow_som_np	N:P ratio for microbial residue pool initialization	g g <sup>-1</sup>	14	21	Reduce P in system
Microbial_cn	Microbial N:C ratio	g g <sup>-1</sup>	7.6	4.3	Pihlblad et al., 2019
Microbial_np	Microbial N:P ratio	g g <sup>-1</sup>	5.6	4.1	Pihlblad et al., 2019; Jiang et al., 2020; Jiang et al., 2024
Qmx_org_fp	maximum sorption capacity of OM to fine soil particle	molC (kg fine particle) <sup>-1</sup>	6.5537	5.57	Reduce organic matter sorption to account for



					soils at EucFACE
km_mic_biochem_ po4	Half-saturation microbial biomass for PO <sub>4</sub> biochemical mineralization	molC m <sup>-3</sup>	0.42	12.49	Account for P- limited soils
<b>vegetation</b>					
Jmax2vcmax_C3	ratio of Jmax25/Vcmax25 for prescribed leaf N	[unitless]	1.92	1.64	Jiang et al., 2024
Root2leaf_cn	relative C: N of fine roots compared to leaves	[unitless]	0.85	0.62	Jiang et al., 2024
lambda_sinklim_PS	Weibull parameter for sink limitation	[unitless]	0.1	0.05	Reduced sink limitation to allow for root exudation
Wood2leaf_cn	relative C: N of sapwood biomass compared to leaves	[unitless]	0.145	0.32	Jiang et al., 2024
Root2leaf_np	relative N:P of fine roots compared to leaves	[unitless]	0.8	1.0	Jiang et al., 2024
Wood2leaf_np	relative N:P of sapwood biomass compared to leaves	[unitless]	0.64	1.0	Jiang et al., 2024





SLA	specific leaf area	mm (mg DW) <sup>-1</sup>	8.99	6.01	Jiang et al., 2024
K_crtos	coarse root to sapwood mass ratio	[unitless]	0.4	0.1	Jiang et al., 2024
K_rtos	trade-off parameter for hydraulic investment into sapwood or fine roots	[unitless]	5.615	4.925	Adjusted to follow allocation in Jiang et al., 2020
K_latosa	leaf area to sapwood area ratio	[unitless]	4000	3000	Adjusted follow allocation in Jiang et al., 2020
Tau_fine_root	fine root turnover	yr	0.75	1.5	Jiang et al., 2024

## 5.2 Enabling priming via microbial grazing

When microbes decay, in the model part of biomass is directly recycled as DOM, part enters residue pool. We altered microbial decay, such that for nitrogen an additional part enters solute NH<sub>4</sub> to account for microbial grazing. Original JSM describes element transfer upon microbial turnover as:

$$\eta_{mic \rightarrow dom}^X = \sigma_{recycle}^X * \frac{X_{mic}}{\tau_{mic}} \quad (A1)$$

$$\eta_{mic \rightarrow res}^X = 1 - \eta_{mic \rightarrow dom}^X \quad (A2)$$

Where  $\eta_{mic \rightarrow dom}^X$  [molX m<sup>3</sup> s<sup>-1</sup>] and  $\eta_{mic \rightarrow res}^X$  [molX m<sup>3</sup> s<sup>-1</sup>] are the fluxes from microbial pool to DOM and residue pool, respectively,  $X_{mic}$  [molX m<sup>3</sup>] is the microbial pool and  $\tau_{mic}$  [s] is the microbial turnover time for C, N and P.  $\sigma_{recycle}^X$  [unitless] is a constant recycling fraction for C and P, but flexible for N. Under N limitation microbes recycle up to 66 % of N, depending on microbial nutrient status. Therefore, microbes in need for N under additional growth would increase recycling but not change enzyme allocation. To bypass this, we fixed the recycling factor and simulate the effect of microbial grazing as:



725

$$\eta_{mic \rightarrow dom}^N = \sigma_{recycle}^N * \frac{N_{mic}}{\tau_{mic}} \tag{A3}$$

$$\eta_{mic \rightarrow NH4sol}^N = \sigma_{grazing}^N * \frac{N_{mic}}{\tau_{mic}} \tag{A5}$$

$$\eta_{mic \rightarrow res}^N = 1 - \eta_{mic \rightarrow dom}^N - \eta_{mic \rightarrow NH4sol}^N \tag{A6}$$

Where  $\eta_{mic \rightarrow NH4sol}^N$  [molX m<sup>3</sup> s<sup>-1</sup>] is the grazing flux from microbial pool to soluble NH<sub>4</sub> pool and  $\sigma_{grazing}^N$  [unitless] is the related fraction.

730 **Table A 2: New parameters for microbial decay and recycling**

	Unit	Standard Quincy-JSM	This study
$\sigma_{recycle}^C$	unitless	0.172	0.3
$\sigma_{recycle}^N$	unitless	(0.172-0.66), At least 0.6 if microbes under N limitation	0.4
$\sigma_{recycle}^P$	unitless	0.172	0.5
$\sigma_{grazing}^X$	unitless	-	0.2



## 6 Appendix B: Additional Tables and Figures

735 **Table B 1: Comparison of mean annual of simulated pools ( $\text{gC m}^{-2}$ ) and fluxes ( $\text{gC m}^{-2} \text{yr}^{-1}$ ) for EucFACE under ambient conditions with observed means and  $\pm$  one standard deviation across 3 rings (2013-2016). NEP refers to 3 different alternative methods of estimation (Jiang et al., 2020; Jiang et al., 2024a)**

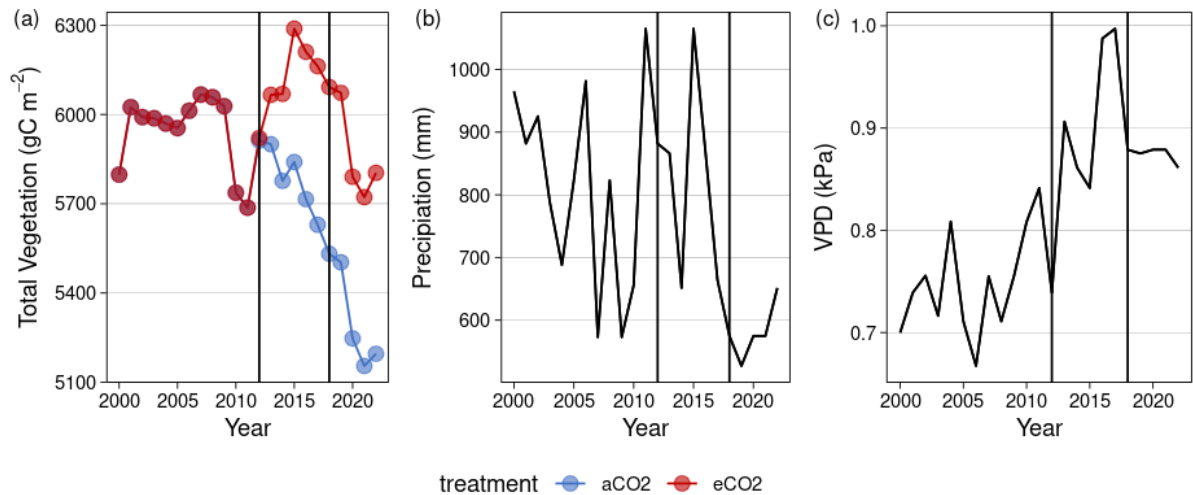
Carbon pool ( $\text{gC m}^{-2}$ )	observed	simulated
Leaf	151 ( $\pm 14$ )	145
Wood	4558 ( $\pm 321$ )	4218
Fine root	227 ( $\pm 5$ )	182
Coarse root	606 ( $\pm 60$ )	622
Soil carbon	2.183 ( $\pm 280$ ) (top 10 cm)	2456(top 13 cm)
Microbial carbon	61 ( $\pm 3.6$ )	81
Carbon flux ( $\text{gC m}^{-2} \text{yr}^{-1}$ )	observed	simulated
Overstorey GPP	1563 ( $\pm 200$ )	1702
NEP	-73 - 28	1
Biomass production	484 ( $\pm 63$ )	365

740 **Table B 2: Comparison of mean annual of simulated pool stoichiometry for EucFACE under ambient conditions with observations (2013-2016) (Jiang et al., 2024a)**

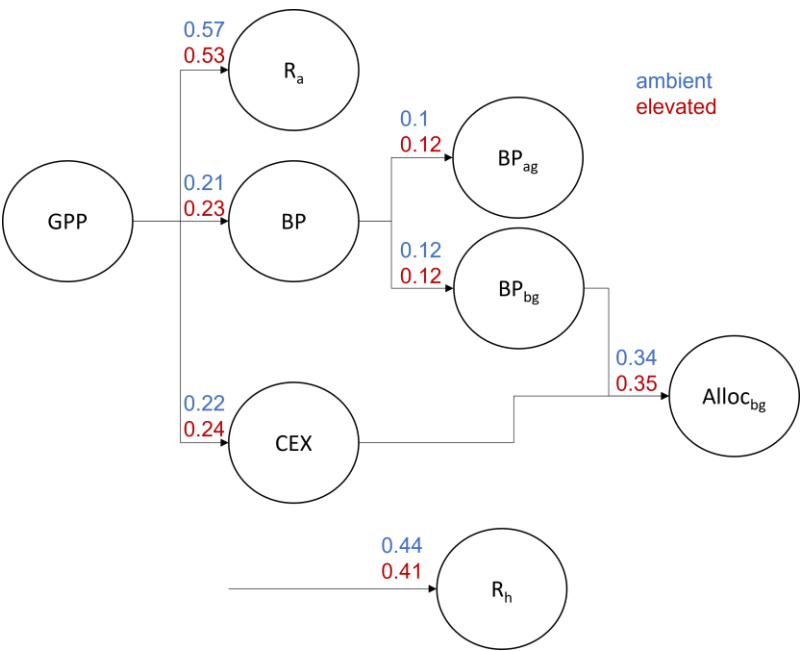
Variable	Observed CN	Simulated CN	Observed NP	Simulated NP
leaf	$35.5 \pm 2.7$	29.6	$22.9 \pm 0.1$	24.4
sapwood	$101.6 \pm 14.7$	110.9	$35.6 \pm 2.1$	35.8
wood	$110.2 \pm 30.3$	138.7	$33.7 \pm 2.7$	35.8
fineroot	$56.9 \pm 4.6$	47.7	$28.7 \pm 3.3$	30.5
soil	$13.8 \pm 1.0$	11.9	$16.4 \pm 3.4$	16.2

745 **Table B 3: Observed (2013-2016) and simulated (2013-2019  $\text{CO}_2$  effect on ecosystem fluxes at EucFACE. Our model did not include understorey. Observed values refer to overstorey gross primary productivity (GPPo), biomass production on aboveground overstorey and whole vegetation root biomass production (BP), autotrophic respiration on aboveground overstorey and whole vegetation root respiration (AutResp), heterotrophic respiration (HetResp) and soil respiration (Rsoil). Observed values from Jiang et al 2020.**

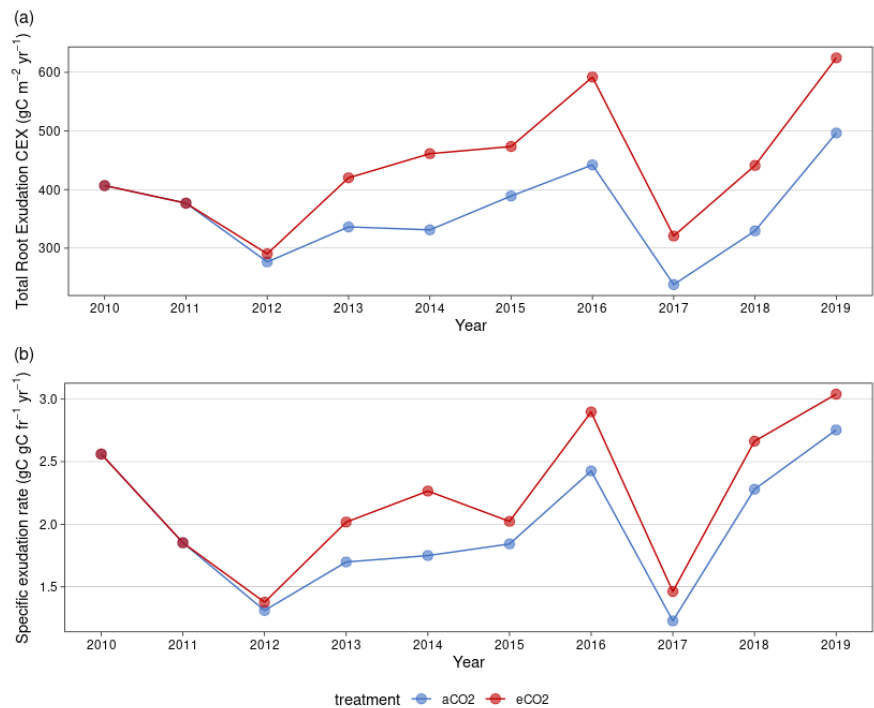
Carbon Flux	Observed increase	Simulated increase
GPPo	12 %	22 %
BP	3 %	33 %
AutResp	5 %	13 %
HetResp	17 %	14 %
Rsoil	12 %	13 %



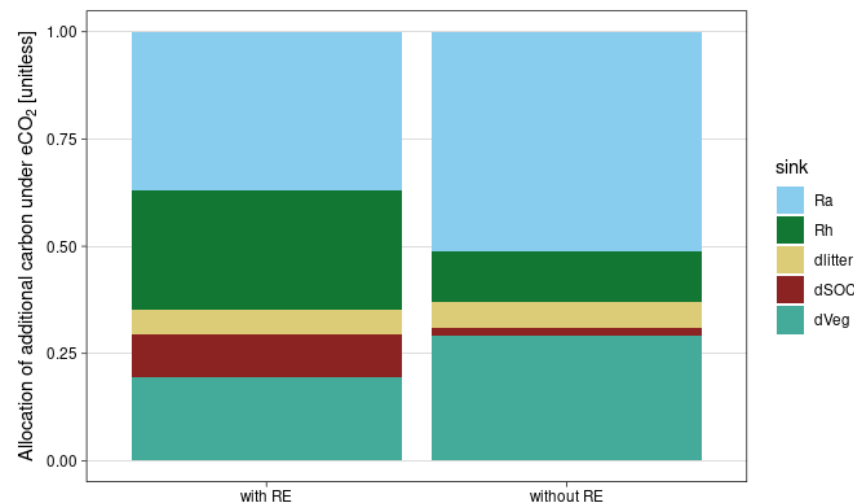
750 **Figure B 1: Simulated total vegetation C, precipitation and vapor pressure deficit (VPD) from 2012 to 2022 for EucFACE under ambient conditions. Vegetation follows a downward trend from 2010-2022 due to climate extremes. Forcing from 2012-2018 (black bars) follows meteorological data observations, while forcing before and after this period follows repeated and randomized observations.**



755 **Figure B 2: Simulated allocation of GPP under ambient and elevated CO2 treatment for EucFACE based on simulated annual mean of fluxes from 2012-2019. Numbers on arrows refer to fraction of GPP. GPP is allocated to autotrophic respiration ( $R_a$ ), biomass production (BP), including aboveground ( $BP_{ag}$ ) and belowground ( $BP_{bg}$ ) biomass production and carbon root exudation (CEX). CEX and  $BP_{bg}$  add up to total belowground allocation. Additionally, the fraction of GPP that is respired via heterotrophic respiration ( $R_h$ ) is shown. (**



760 **Figure B 3: Simulated total root exudation for 2010 to 2019 for EucFACE for ambient and elevated treatment as (a) Total root exudation flux and (b) Specific root exudation rate. CO<sub>2</sub> fumigation started with ramp up end of 2012.**



765 **Figure B 4: Simulated allocation of additional GPP under eCO<sub>2</sub> with root exudation module (with RE) and without root exudation module (without RE) for 2013-2029. Additional GPP can be allocated into autotroph respiration (Ra), heterotrophic respiration (Rh), litter (dLitter), soil organic carbon (dSOC) or vegetation carbon (dVeg)**

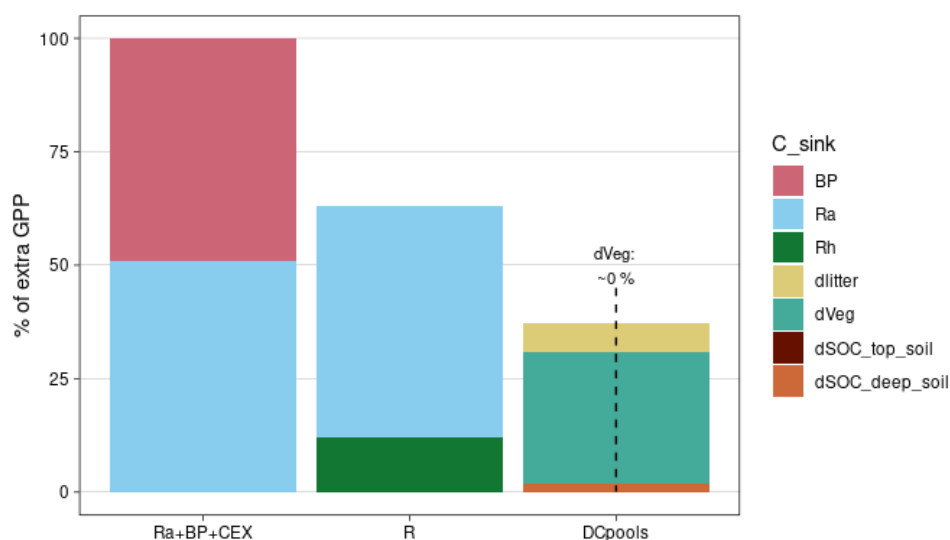
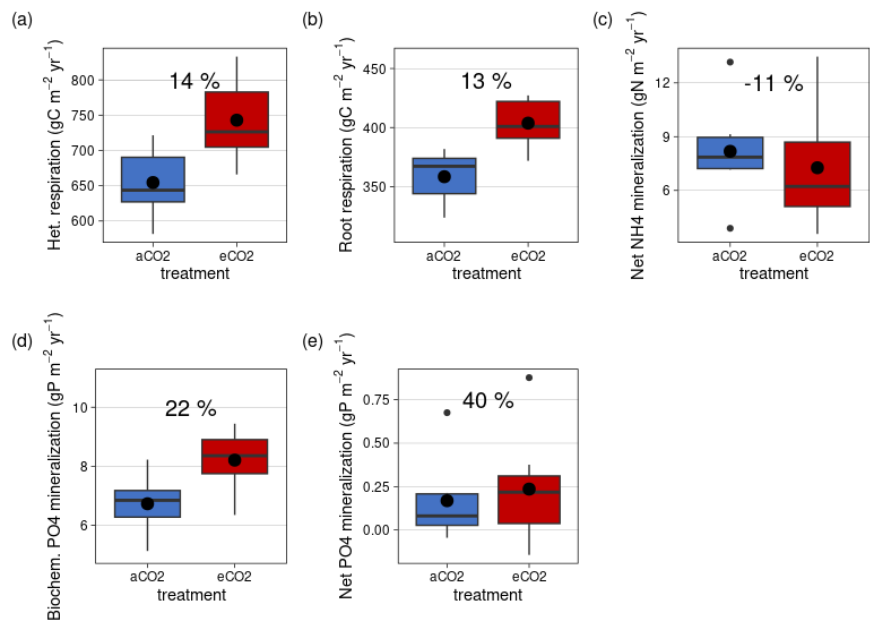
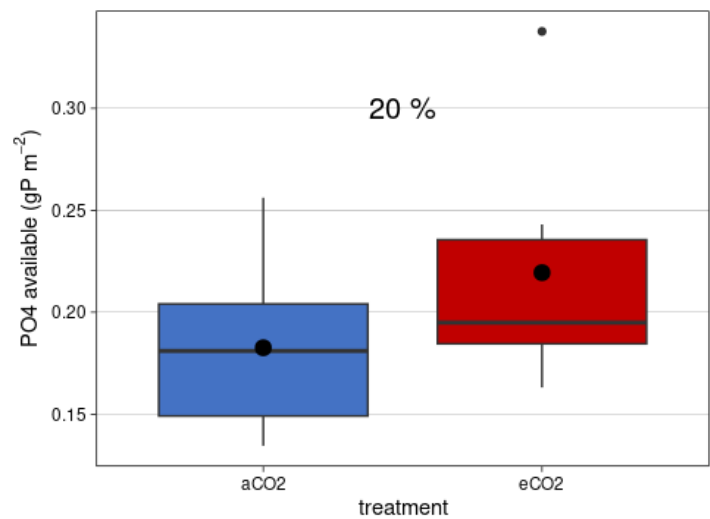


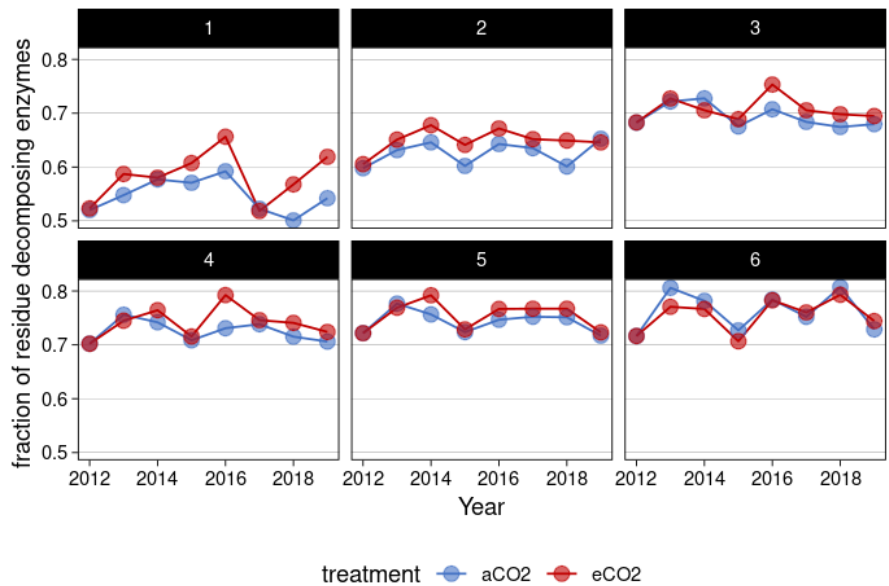
**Figure B 5:** Simulated fate of additional sequestered C under eCO<sub>2</sub> as percentage of increased overstorey gross primary productivity (GPP) for simulations without root exudation (2013-2019). For simulations additional GPP is transferred into autotrophic respiration (Ra), biomass production (BP). Ecosystem respiration (R) is composed of heterotrophic respiration (Rh) and autotrophic respiration (Ra). Change in ecosystem carbon pools is composed of change in topsoil organic C (dSOC\_top\_soil top 10 cm for observation, top 50 cm for simulation), change in deep soil SOC (dSOC\_deep\_soil, no observations) change in litter (dlitter) and change in vegetation (dVeg).



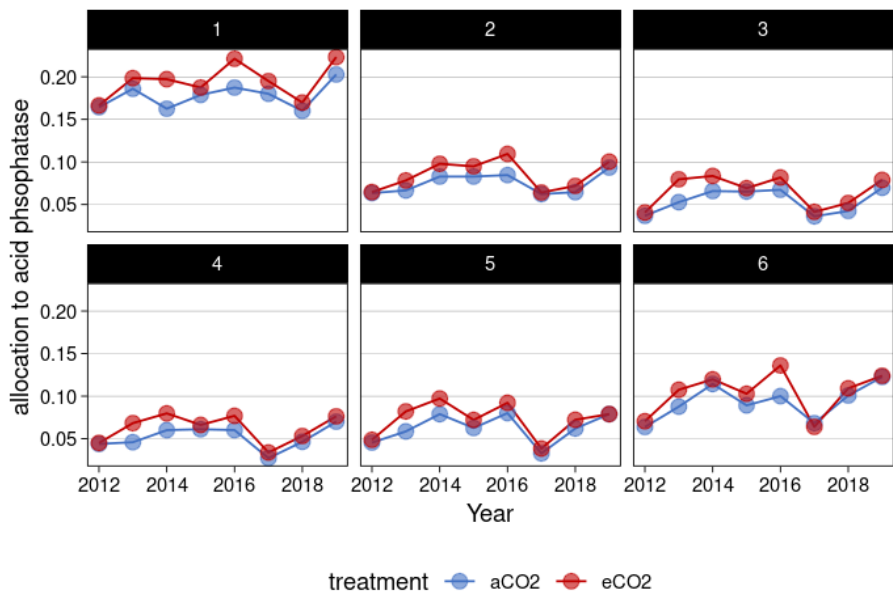
775 **Figure B 6: Simulated major mineralization fluxes for C, N and P under ambient and elevated CO<sub>2</sub> (2013-2019) for topsoil layers. (a) Heterotrophic respiration, (b) Root respiration, (c) Net NH<sub>4</sub> mineralization, (d) biochemical mineralization, (e) Net PO<sub>4</sub> mineralization as sum of biological and biochemical mineralization. Boxplots show annual variation of fluxes, dots represent mean values. Percentage difference based on Annual mean for 2013-2019 is given for each flux.**



780 **Figure B 7: Mean annual available PO<sub>4</sub> for plant and microbial uptake under ambient and elevated conditions in topsoil for 7 years of simulation (2013-2019). Boxplots show annual variation of fluxes, dots represent mean values. Percentage difference based on annual mean for 2013-2019 is shown above boxplots.**



785 **Figure B 8: Simulated fraction of residue decomposing enzymes for top 6 soil layers (topsoil) in QUINCY-JSM for EucFACE**  
under ambient and elevated conditions (2013-2019).



790 **Figure B 9: Simulated acid phosphatase allocation in microbes for top 6 soil layers (topsoil) in QUINCY-JSM JSM for EucFACE**  
under ambient and elevated conditions (2013-2019).



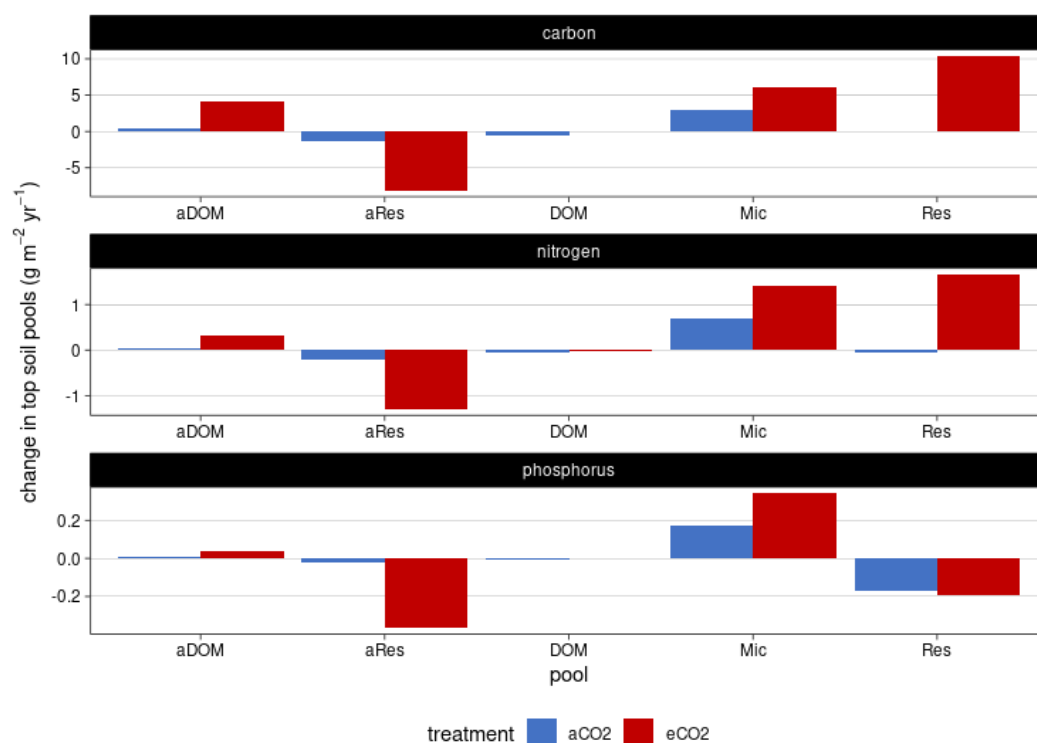


**Figure B 10: Simulated changes in topsoil pools for EucFACE under ambient and elevated CO<sub>2</sub> treatment 2013-2019: ineral associated DOM (aDOM), mineral associated microbial residue (aRes), dissolved organic matter (DOM), microbes (Mic) and microbial residue (Res).**

795

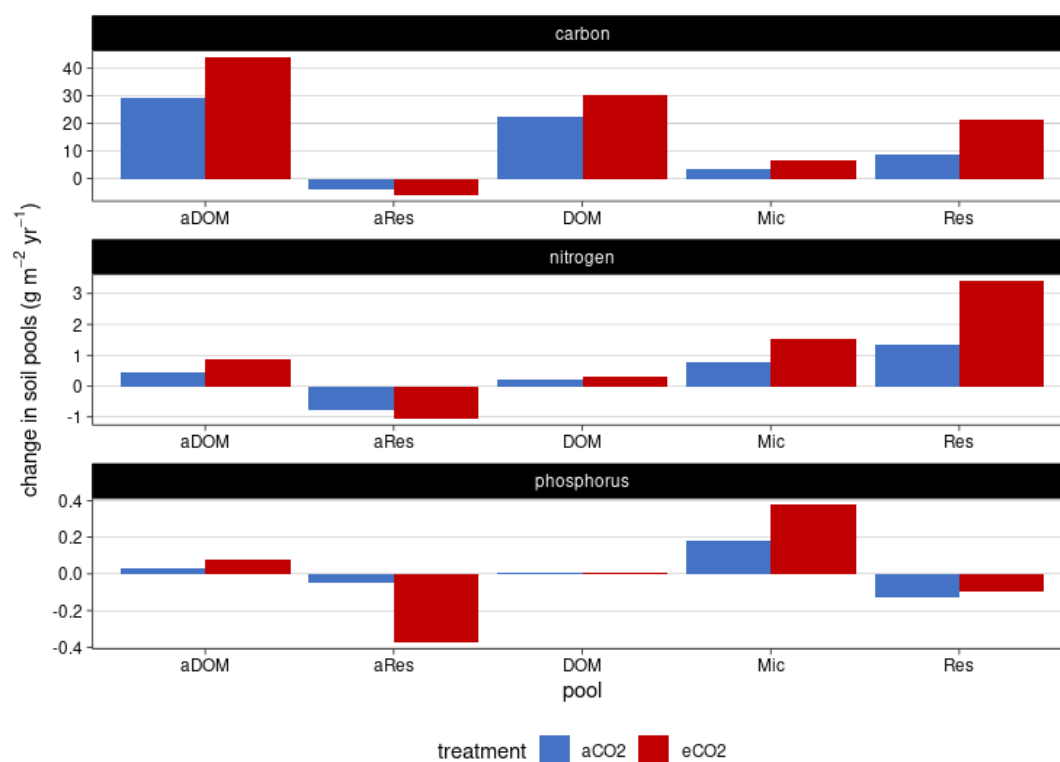


**Figure B 11: Simulated changes in soil pools for whole soil column for EucFACE under ambient and elevated CO<sub>2</sub> treatment 2013-2019: mineral associated DOM (aDOM), mineral associated microbial residue (aRes), dissolved organic matter (DOM), microbes (Mic) and microbial residue (Res)**

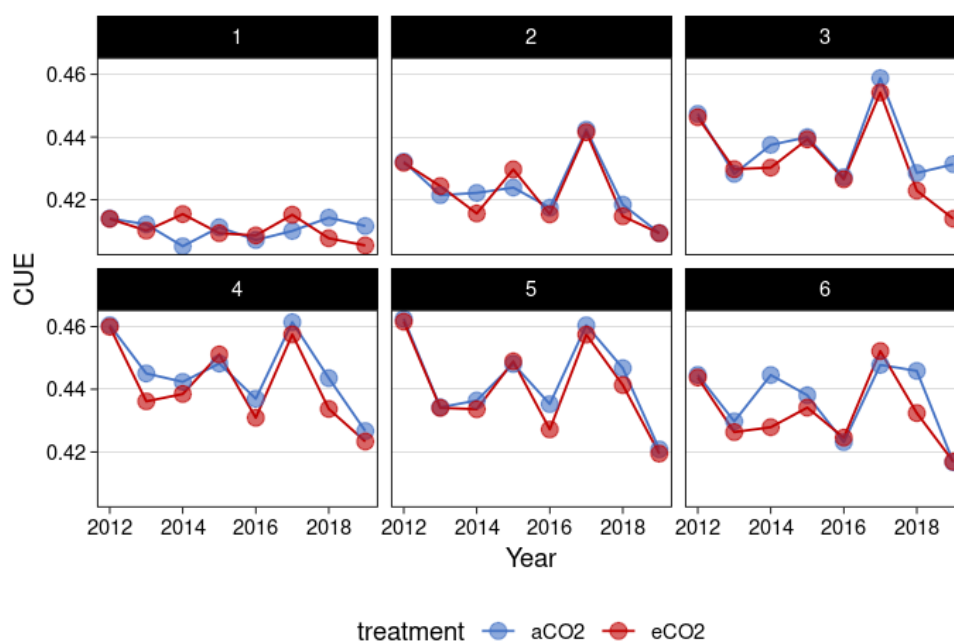


**Figure B 12: Simulated microbial carbon use efficiency for top 6 soil layers (topsoil) in QUINCY-JSM JSM for EucFACE under ambient and elevated conditions (2013-2019).**



**Code availability.** The model is open source under the GNU GPL v3 and MPI-M ICON software license agreement (depending on module). The code is available under <https://doi.org/10.17871/quincy-model-2019>. A copy of the scientific code can be found in this temporary (01.12.2025) private link for review purposes:

<https://nextcloud.bgc-jena.mpg.de/s/w2EiXdBDZmGX4F9>.

810 Forcing data to run the model for testbed simulations can be made available on request.

**Competing interests.** At least one of the (co-)authors is a member of the editorial board of Biogeosciences

**Acknowledgement:** KS acknowledges financial support from the IMPRS for Global Biogeochemical Cycles.

815

**Contribution of authors.** KS, KF and SZ designed the study. KS, KF and SZ interpreted the results. KS wrote model implementation and first draft of the manuscript. KF, AR, LY, MJ, BEM, SZ contributed to manuscript revision.

**Additional Licences.** Two figures were made with Biorender.com. The licenses can be found with the following links:

820 <https://biorender.com/7hbj3d>

<https://biorender.com/b5hxuaa>



## 7 References

- 825 Ai, J., Banfield, C. C., Shao, G., Zamanian, K., Stürzebecher, T., Shi, L., Fan, L., Liu, X., Spielvogel, S., and Dippold, M. A.: What controls the availability of organic and inorganic P sources in top- and subsoils? A  $^{33}\text{P}$  isotopic labeling study with root exudate addition, *Soil Biology and Biochemistry*, 185, 109129, <https://doi.org/10.1016/j.soilbio.2023.109129>, 2023.
- Akatsuki, M. and Makita, N.: Influence of fine root traits on in situ exudation rates in four conifers from different mycorrhizal associations, *Tree Physiology*, 40, 1071–1079, <https://doi.org/10.1093/treephys/tpaa051>, 2020.
- 830 Ataka, M., Sun, L., Nakaji, T., Katayama, A., and Hiura, T.: Five-year nitrogen addition affects fine root exudation and its correlation with root respiration in a dominant species, *Quercus crispula*, of a cool temperate forest, Japan, *Tree Physiology*, 40, 367–376, <https://doi.org/10.1093/treephys/tpz143>, 2020.
- Atkin, O. K., Meir, P., and Turnbull, M. H.: Improving representation of leaf respiration in large-scale predictive climate–vegetation models, *New Phytologist*, 202, 743–748, <https://doi.org/10.1111/nph.12686>, 2014.
- 835 Bastida, F., García, C., Fierer, N., Eldridge, D. J., Bowker, M. A., Abades, S., Alfaro, F. D., Asefaw Berhe, A., Cutler, N. A., Gallardo, A., García-Velázquez, L., Hart, S. C., Hayes, P. E., Hernández, T., Hseu, Z.-Y., Jehmlich, N., Kirchmair, M., Lambers, H., Neuhauser, S., Peña-Ramírez, V. M., Pérez, C. A., Reed, S. C., Santos, F., Siebe, C., Sullivan, B. W., Trivedi, P., Vera, A., Williams, M. A., Luis Moreno, J., and Delgado-Baquerizo, M.: Global ecological predictors of the soil priming effect, *Nat Commun*, 10, 3481, <https://doi.org/10.1038/s41467-019-11472-7>, 2019.
- 840 Brunn, M., Hafner, B. D., Zwetsloot, M. J., Weigl, F., Pritsch, K., Hikino, K., Ruehr, N. K., Sayer, E. J., and Bauerle, T. L.: Carbon allocation to root exudates is maintained in mature temperate tree species under drought, *New Phytologist*, 235, 965–977, <https://doi.org/10.1111/nph.18157>, 2022.
- Castañeda-Gómez, L., Walker, J. K. M., Powell, J. R., Ellsworth, D. S., Pendall, E., and Carrillo, Y.: Impacts of elevated carbon dioxide on carbon gains and losses from soil and associated microbes in a *Eucalyptus* woodland, *Soil Biology and Biochemistry*, 143, 107734, <https://doi.org/10.1016/j.soilbio.2020.107734>, 2020.
- 845 Chari, N. R., Tumber-Dávila, S. J., Phillips, R. P., Bauerle, T. L., Brunn, M., Hafner, B. D., Klein, T., Obersteiner, S., Reay, M. K., Ullah, S., and Taylor, B. N.: Estimating the global root exudate carbon flux, *Biogeochemistry*, 167, 895–908, <https://doi.org/10.1007/s10533-024-01161-z>, 2024.
- Chertov, O., Kuzyakov, Y., Pripulina, I., Frolov, P., Shanin, V., and Grabarnik, P.: Modelling the Rhizosphere Priming Effect in Combination with Soil Food Webs to Quantify Interaction between Living Plant, Soil Biota and Soil Organic Matter, *Plants*, 11, 2605, <https://doi.org/10.3390/plants11192605>, 2022.
- Cotrufo, M. F., Wallenstein, M. D., Boot, C. M., Denef, K., and Paul, E.: The Microbial Efficiency-Matrix Stabilization (MEMS) framework integrates plant litter decomposition with soil organic matter stabilization: do labile plant inputs form stable soil organic matter?, *Global Change Biology*, 19, 988–995, <https://doi.org/10.1111/gcb.12113>, 2013.
- 855 Crous, K. Y., Ósváldsson, A., and Ellsworth, D. S.: Is phosphorus limiting in a mature *Eucalyptus* woodland? Phosphorus fertilisation stimulates stem growth, *Plant Soil*, 391, 293–305, <https://doi.org/10.1007/s11104-015-2426-4>, 2015.



- De Andrade, S. A. L., Borghi, A. A., De Oliveira, V. H., Gouveia, L. de M., Martins, A. P. I., and Mazzafera, P.: Phosphorus Shortage Induces an Increase in Root Exudation in Fifteen Eucalypts Species, *Agronomy*, 12, 2041, <https://doi.org/10.3390/agronomy12092041>, 2022.
- 860 De Kauwe, M. G., Medlyn, B. E., Zaehle, S., Walker, A. P., Dietze, M. C., Wang, Y.-P., Luo, Y., Jain, A. K., El-Masri, B., Hickler, T., Wårlind, D., Weng, E., Parton, W. J., Thornton, P. E., Wang, S., Prentice, I. C., Asao, S., Smith, B., McCarthy, H. R., Iversen, C. M., Hanson, P. J., Warren, J. M., Oren, R., and Norby, R. J.: Where does the carbon go? A model–data intercomparison of vegetation carbon allocation and turnover processes at two temperate forest free-air CO<sub>2</sub> enrichment sites, *New Phytologist*, 203, 883–899, <https://doi.org/10.1111/nph.12847>, 2014.
- 865 Dijkstra, F., Carrillo, Y., Pendall, E., and Morgan, J.: Rhizosphere priming: a nutrient perspective, *Frontiers in Microbiology*, 4, 2013.
- Drake, J. E., Gallet-Budynek, A., Hofmockel, K. S., Bernhardt, E. S., Billings, S. A., Jackson, R. B., Johnsen, K. S., Lichter, J., McCarthy, H. R., McCormack, M. L., Moore, D. J. P., Oren, R., Palmroth, S., Phillips, R. P., Pippen, J. S., Pritchard, S. G., Treseder, K. K., Schlesinger, W. H., DeLucia, E. H., and Finzi, A. C.: Increases in the flux of carbon belowground stimulate
- 870 nitrogen uptake and sustain the long-term enhancement of forest productivity under elevated CO<sub>2</sub>, *Ecology Letters*, 14, 349–357, <https://doi.org/10.1111/j.1461-0248.2011.01593.x>, 2011.
- Drake, J. E., Macdonald, C. A., Tjoelker, M. G., Crous, K. Y., Gimeno, T. E., Singh, B. K., Reich, P. B., Anderson, I. C., and Ellsworth, D. S.: Short-term carbon cycling responses of a mature eucalypt woodland to gradual stepwise enrichment of atmospheric CO<sub>2</sub> concentration, *Global Change Biology*, 22, 380–390, <https://doi.org/10.1111/gcb.13109>, 2016.
- 875 Drake, J. E., Macdonald, C. A., Tjoelker, M. G., Reich, P. B., Singh, B. K., Anderson, I. C., and Ellsworth, D. S.: Three years of soil respiration in a mature eucalypt woodland exposed to atmospheric CO<sub>2</sub> enrichment, *Biogeochemistry*, 139, 85–101, <https://doi.org/10.1007/s10533-018-0457-7>, 2018.
- Du, E., Terrer, C., Pellegrini, A. F. A., Ahlström, A., van Lissa, C. J., Zhao, X., Xia, N., Wu, X., and Jackson, R. B.: Global patterns of terrestrial nitrogen and phosphorus limitation, *Nat. Geosci.*, 13, 221–226, <https://doi.org/10.1038/s41561-019-0530-4>, 2020.
- 880 Ellsworth, D. S., Anderson, I. C., Crous, K. Y., Cooke, J., Drake, J. E., Gherlenda, A. N., Gimeno, T. E., Macdonald, C. A., Medlyn, B. E., Powell, J. R., Tjoelker, M. G., and Reich, P. B.: Elevated CO<sub>2</sub> does not increase eucalypt forest productivity on a low-phosphorus soil, *Nature Clim Change*, 7, 279–282, <https://doi.org/10.1038/nclimate3235>, 2017.
- Filion, M., Dutilleul, P., and Potvin, C.: Optimum experimental design for Free-Air Carbon dioxide Enrichment (FACE) studies, *Global Change Biology*, 6, 843–854, <https://doi.org/10.1046/j.1365-2486.2000.00353.x>, 2000.
- 885 Finzi, A. C., Norby, R. J., Calfapietra, C., Gallet-Budynek, A., Gielen, B., Holmes, W. E., Hoosbeek, M. R., Iversen, C. M., Jackson, R. B., Kubiske, M. E., Ledford, J., Liberloo, M., Oren, R., Polle, A., Pritchard, S., Zak, D. R., Schlesinger, W. H., and Ceulemans, R.: Increases in nitrogen uptake rather than nitrogen-use efficiency support higher rates of temperate forest productivity under elevated CO<sub>2</sub>, *Proceedings of the National Academy of Sciences*, 104, 14014–14019, <https://doi.org/10.1073/pnas.0706518104>, 2007.
- 890



- Fleischer, K., Rammig, A., De Kauwe, M. G., Walker, A. P., Domingues, T. F., Fuchslueger, L., Garcia, S., Goll, D. S., Grandis, A., Jiang, M., Haverd, V., Hofhansl, F., Holm, J. A., Kruijt, B., Leung, F., Medlyn, B. E., Mercado, L. M., Norby, R. J., Pak, B., von Randow, C., Quesada, C. A., Schaap, K. J., Valverde-Barrantes, O. J., Wang, Y.-P., Yang, X., Zaehle, S., Zhu, Q., and Lapola, D. M.: Amazon forest response to CO<sub>2</sub> fertilization dependent on plant phosphorus acquisition, *Nat. Geosci.*, 12, 736–741, <https://doi.org/10.1038/s41561-019-0404-9>, 2019.
- 895 Friend, A. D. and Kiang, N. Y.: Land Surface Model Development for the GISS GCM: Effects of Improved Canopy Physiology on Simulated Climate, *Journal of Climate*, 18, 2883–2902, <https://doi.org/10.1175/JCLI3425.1>, 2005.
- Grant, R. F.: Modelling changes in nitrogen cycling to sustain increases in forest productivity under elevated atmospheric CO<sub>2</sub> and contrasting site conditions, *Biogeosciences*, 10, 7703–7721, <https://doi.org/10.5194/bg-10-7703-2013>, 2013.
- 900 van Groenigen, K. J., Qi, X., Osenberg, C. W., Luo, Y., and Hungate, B. A.: Faster Decomposition Under Increased Atmospheric CO<sub>2</sub> Limits Soil Carbon Storage, *Science*, 344, 508–509, <https://doi.org/10.1126/science.1249534>, 2014.
- van Groenigen, K. J., Osenberg, C. W., Terrer, C., Carrillo, Y., Dijkstra, F. A., Heath, J., Nie, M., Pendall, E., Phillips, R. P., and Hungate, B. A.: Faster turnover of new soil carbon inputs under increased atmospheric CO<sub>2</sub>, *Global Change Biology*, 23, 4420–4429, <https://doi.org/10.1111/gcb.13752>, 2017.
- 905 Hasegawa, S., Macdonald, C. A., and Power, S. A.: Elevated carbon dioxide increases soil nitrogen and phosphorus availability in a phosphorus-limited Eucalyptus woodland, *Global Change Biology*, 22, 1628–1643, <https://doi.org/10.1111/gcb.13147>, 2016.
- Hasegawa, S., Ryan, M. H., and Power, S. A.: CO<sub>2</sub> concentration and water availability alter the organic acid composition of root exudates in native Australian species, *Plant Soil*, 485, 507–524, <https://doi.org/10.1007/s11104-022-05845-z>, 2023.
- 910 Hedley, M. J., Stewart, J. W. B., and Chauhan, B. S.: Changes in Inorganic and Organic Soil Phosphorus Fractions Induced by Cultivation Practices and by Laboratory Incubations, *Soil Science Society of America Journal*, 46, 970–976, <https://doi.org/10.2136/sssaj1982.03615995004600050017x>, 1982.
- Helfenstein, J., Ringeval, B., Tamburini, F., Mulder, V. L., Goll, D. S., He, X., Alblas, E., Wang, Y., Mollier, A., and Frossard, E.: Understanding soil phosphorus cycling for sustainable development: A review, *One Earth*, 7, 1727–1740, <https://doi.org/10.1016/j.oneear.2024.07.020>, 2024.
- 915 Hinsinger, P.: Bioavailability of soil inorganic P in the rhizosphere as affected by root-induced chemical changes: a review, *Plant and Soil*, 237, 173–195, <https://doi.org/10.1023/A:1013351617532>, 2001.
- Jiang, M., Zaehle, S., De Kauwe, M. G., Walker, A. P., Caldararu, S., Ellsworth, D. S., and Medlyn, B. E.: The quasi-equilibrium framework revisited: analyzing long-term CO<sub>2</sub> enrichment responses in plant–soil models, *Geoscientific Model Development*, 12, 2069–2089, <https://doi.org/10.5194/gmd-12-2069-2019>, 2019.
- 920 Jiang, M., Medlyn, B. E., Drake, J. E., Duursma, R. A., Anderson, I. C., Barton, C. V. M., Boer, M. M., Carrillo, Y., Castañeda-Gómez, L., Collins, L., Crous, K. Y., De Kauwe, M. G., dos Santos, B. M., Emmerson, K. M., Facey, S. L., Gherlenda, A. N., Gimeno, T. E., Hasegawa, S., Johnson, S. N., Kännaste, A., Macdonald, C. A., Mahmud, K., Moore, B. D., Nazaries, L., Neilson, E. H. J., Nielsen, U. N., Niinemets, Ü., Noh, N. J., Ochoa-Hueso, R., Pathare, V. S., Pendall, E., Pihlblad, J., Piñeiro,



- 925 J., Powell, J. R., Power, S. A., Reich, P. B., Renchon, A. A., Riegler, M., Rinnan, R., Rymer, P. D., Salomón, R. L., Singh, B. K., Smith, B., Tjoelker, M. G., Walker, J. K. M., Wujeska-Klaue, A., Yang, J., Zaehle, S., and Ellsworth, D. S.: The fate of carbon in a mature forest under carbon dioxide enrichment, *Nature*, 580, 227–231, <https://doi.org/10.1038/s41586-020-2128-9>, 2020.
- Jiang, M., Medlyn, B. E., Wårlind, D., Knauer, J., Fleischer, K., Goll, D. S., Olin, S., Yang, X., Yu, L., Zaehle, S., Zhang, H.,  
930 Lv, H., Crous, K. Y., Carrillo, Y., Macdonald, C., Anderson, I., Boer, M. M., Farrell, M., Gherlenda, A., Castañeda-Gómez, L., Hasegawa, S., Jarosch, K., Milham, P., Ochoa-Hueso, R., Pathare, V., Pihlblad, J., Nevado, J. P., Powell, J., Power, S. A., Reich, P., Riegler, M., Ellsworth, D. S., and Smith, B.: Carbon-phosphorus cycle models overestimate CO<sub>2</sub> enrichment response in a mature Eucalyptus forest, *Science Advances*, 10, ead15822, <https://doi.org/10.1126/sciadv.ad15822>, 2024a.
- Jiang, M., Crous, K. Y., Carrillo, Y., Macdonald, C. A., Anderson, I. C., Boer, M. M., Farrell, M., Gherlenda, A. N., Castañeda-  
935 Gómez, L., Hasegawa, S., Jarosch, K., Milham, P. J., Ochoa-Hueso, R., Pathare, V., Pihlblad, J., Piñeiro, J., Powell, J. R., Power, S. A., Reich, P. B., Riegler, M., Zaehle, S., Smith, B., Medlyn, B. E., and Ellsworth, D. S.: Microbial competition for phosphorus limits the CO<sub>2</sub> response of a mature forest, *Nature*, 1–6, <https://doi.org/10.1038/s41586-024-07491-0>, 2024b.
- Jiang, Z., Thakur, M. P., Liu, R., Zhou, G., Zhou, L., Fu, Y., Zhang, P., He, Y., Shao, J., Gao, J., Li, N., Wang, X., Jia, S., Chen, Y., Zhang, C., and Zhou, X.: Soil P availability and mycorrhizal type determine root exudation in sub-tropical forests,  
940 *Soil Biology and Biochemistry*, 171, 108722, <https://doi.org/10.1016/j.soilbio.2022.108722>, 2022.
- Jones, D. L., Hodge, A., and Kuzyakov, Y.: Plant and mycorrhizal regulation of rhizodeposition, *New Phytologist*, 163, 459–480, <https://doi.org/10.1111/j.1469-8137.2004.01130.x>, 2004.
- Kästner, M., Miltner, A., Thiele-Bruhn, S., and Liang, C.: Microbial Necromass in Soils—Linking Microbes to Soil Processes and Carbon Turnover, *Frontiers in Environmental Science*, 9, 2021.
- 945 Kull, O. and Kruijt, B.: Leaf photosynthetic light response: a mechanistic model for scaling photosynthesis to leaves and canopies, *Functional Ecology*, 12, 767–777, <https://doi.org/10.1046/j.1365-2435.1998.00257.x>, 1998.
- Kuzyakov, Y., Horwath, W. R., Dorodnikov, M., and Blagodatskaya, E.: Review and synthesis of the effects of elevated atmospheric CO<sub>2</sub> on soil processes: No changes in pools, but increased fluxes and accelerated cycles, *Soil Biol. Biochem.*, 128, 66–78, <https://doi.org/10.1016/j.soilbio.2018.10.005>, 2019.
- 950 Lambers, H.: Phosphorus Acquisition and Utilization in Plants, *Annu. Rev. Plant Biol.*, 73, 17–42, <https://doi.org/10.1146/annurev-arplant-102720-125738>, 2022.
- Leuschner, C., Tüchtemann, T., and Meier, I. C.: Temperature effects on root exudation in mature beech (*Fagus sylvatica* L.) forests along an elevational gradient, *Plant Soil*, <https://doi.org/10.1007/s11104-022-05629-5>, 2022.
- Li, Z., Liu, Z., Gao, G., Yang, X., and Gu, J.: Shift from Acquisitive to Conservative Root Resource Acquisition Strategy  
955 Associated with Increasing Tree Age: A Case Study of *Fraxinus mandshurica*, *Forests*, 12, 1797, <https://doi.org/10.3390/f12121797>, 2021.
- Liang, C., Schimel, J. P., and Jastrow, J. D.: The importance of anabolism in microbial control over soil carbon storage, *Nat Microbiol*, 2, 1–6, <https://doi.org/10.1038/nmicrobiol.2017.105>, 2017.





- Liang, C., Amelung, W., Lehmann, J., and Kästner, M.: Quantitative assessment of microbial necromass contribution to soil  
960 organic matter, *Global Change Biology*, 25, 3578–3590, <https://doi.org/10.1111/gcb.14781>, 2019.
- Lloyd, J. and Taylor, J. A.: On the Temperature Dependence of Soil Respiration, *Functional Ecology*, 8, 315,  
<https://doi.org/10.2307/2389824>, 1994.
- Lopez-Sangil, L., George, C., Medina-Barcenas, E., Birkett, A. J., Baxendale, C., Bréchet, L. M., Estradera-Gumbau, E., and  
Sayer, E. J.: The Automated Root Exudate System (ARES): a method to apply solutes at regular intervals to soils in the field,  
965 *Methods in Ecology and Evolution*, 8, 1042–1050, <https://doi.org/10.1111/2041-210X.12764>, 2017.
- Manzoni, S., Taylor, P., Richter, A., Porporato, A., and Ågren, G. I.: Environmental and stoichiometric controls on microbial  
carbon-use efficiency in soils, *New Phytologist*, 196, 79–91, <https://doi.org/10.1111/j.1469-8137.2012.04225.x>, 2012.
- Margalef, O., Sardans, J., Fernández-Martínez, M., Molowny-Horas, R., Janssens, I. A., Ciais, P., Goll, D., Richter, A.,  
Obersteiner, M., Asensio, D., and Peñuelas, J.: Global patterns of phosphatase activity in natural soils, *Sci Rep*, 7, 1337,  
970 <https://doi.org/10.1038/s41598-017-01418-8>, 2017.
- Marklein, A. R. and Houlton, B. Z.: Nitrogen inputs accelerate phosphorus cycling rates across a wide variety of terrestrial  
ecosystems, *New Phytologist*, 193, 696–704, <https://doi.org/10.1111/j.1469-8137.2011.03967.x>, 2012.
- McGill, W. B. and Cole, C. V.: Comparative aspects of cycling of organic C, N, S and P through soil organic matter, *Geoderma*,  
26, 267–286, [https://doi.org/10.1016/0016-7061\(81\)90024-0](https://doi.org/10.1016/0016-7061(81)90024-0), 1981.
- 975 McLeod, A. R. and Long, S. P.: Free-air Carbon Dioxide Enrichment (FACE) in Global Change Research: A Review, in:  
*Advances in Ecological Research*, vol. 28, edited by: Fitter, A. H. and Raffaelli, D., Academic Press, 1–56,  
[https://doi.org/10.1016/S0065-2504\(08\)60028-8](https://doi.org/10.1016/S0065-2504(08)60028-8), 1999.
- Medlyn, B. E., De Kauwe, M. G., Zaehle, S., Walker, A. P., Duursma, R. A., Luus, K., Mishurov, M., Pak, B., Smith, B.,  
Wang, Y.-P., Yang, X., Crous, K. Y., Drake, J. E., Gimeno, T. E., Macdonald, C. A., Norby, R. J., Power, S. A., Tjoelker, M.  
980 G., and Ellsworth, D. S.: Using models to guide field experiments: a priori predictions for the CO<sub>2</sub> response of a nutrient- and  
water-limited native Eucalypt woodland, *Global Change Biology*, 22, 2834–2851, <https://doi.org/10.1111/gcb.13268>, 2016.
- Meier, I. C., Tückmantel, T., Heitkötter, J., Müller, K., Preusser, S., Wrobel, T. J., Kandeler, E., Marschner, B., and Leuschner,  
C.: Root exudation of mature beech forests across a nutrient availability gradient: the role of root morphology and fungal  
activity, *New Phytologist*, 226, 583–594, <https://doi.org/10.1111/nph.16389>, 2020.
- 985 Miltner, A., Bombach, P., Schmidt-Brücken, B., and Kästner, M.: SOM genesis: microbial biomass as a significant source,  
*Biogeochemistry*, 111, 41–55, <https://doi.org/10.1007/s10533-011-9658-z>, 2012.
- Nannipieri, P., Giagnoni, L., Landi, L., and Renella, G.: Role of Phosphatase Enzymes in Soil, in: *Phosphorus in Action:  
Biological Processes in Soil Phosphorus Cycling*, edited by: Bünemann, E., Oberson, A., and Frossard, E., Springer, Berlin,  
Heidelberg, 215–243, [https://doi.org/10.1007/978-3-642-15271-9\\_9](https://doi.org/10.1007/978-3-642-15271-9_9), 2011.
- 990 Norby, R. J., DeLucia, E. H., Gielen, B., Calfapietra, C., Giardina, C. P., King, J. S., Ledford, J., McCarthy, H. R., Moore, D.  
J. P., Ceulemans, R., De Angelis, P., Finzi, A. C., Karnosky, D. F., Kubiske, M. E., Lukac, M., Pregitzer, K. S., Scarascia-  
Mugnozza, G. E., Schlesinger, W. H., and Oren, R.: Forest response to elevated CO<sub>2</sub> is conserved across a broad range of



- productivity, *Proceedings of the National Academy of Sciences*, 102, 18052–18056, <https://doi.org/10.1073/pnas.0509478102>, 2005.
- 995 Norby, R. J., Warren, J. M., Iversen, C. M., Medlyn, B. E., and McMurtrie, R. E.: CO<sub>2</sub> enhancement of forest productivity constrained by limited nitrogen availability, *Proceedings of the National Academy of Sciences*, 107, 19368–19373, <https://doi.org/10.1073/pnas.1006463107>, 2010.
- Norby, R. J., Loader, N. J., Mayoral, C., Ullah, S., Curioni, G., Smith, A. R., Reay, M. K., van Wijnngaarden, K., Amjad, M. S., Brettell, D., Crockatt, M. E., Denny, G., Grzesik, R. T., Hamilton, R. L., Hart, K. M., Hartley, I. P., Jones, A. G., Kourmouli, A., Larsen, J. R., Shi, Z., Thomas, R. M., and MacKenzie, A. R.: Enhanced woody biomass production in a mature temperate forest under elevated CO<sub>2</sub>, *Nat. Clim. Chang.*, 14, 983–988, <https://doi.org/10.1038/s41558-024-02090-3>, 2024.
- Ochoa-Hueso, R., Hughes, J., Delgado-Baquerizo, M., Drake, J. E., Tjoelker, M. G., Piñeiro, J., and Power, S. A.: Rhizosphere-driven increase in nitrogen and phosphorus availability under elevated atmospheric CO<sub>2</sub> in a mature *Eucalyptus* woodland, *Plant Soil*, 416, 283–295, <https://doi.org/10.1007/s11104-017-3212-2>, 2017.
- 1005 Pantigoso, H. A., Manter, D. K., Fonte, S. J., and Vivanco, J. M.: Root exudate-derived compounds stimulate the phosphorus solubilizing ability of bacteria, *Sci Rep*, 13, 4050, <https://doi.org/10.1038/s41598-023-30915-2>, 2023.
- Phillips, R. P., Erlitz, Y., Bier, R., and Bernhardt, E. S.: New approach for capturing soluble root exudates in forest soils, *Functional Ecology*, 22, 990–999, <https://doi.org/10.1111/j.1365-2435.2008.01495.x>, 2008.
- Phillips, R. P., Finzi, A. C., and Bernhardt, E. S.: Enhanced root exudation induces microbial feedbacks to N cycling in a pine forest under long-term CO<sub>2</sub> fumigation, *Ecology Letters*, 14, 187–194, <https://doi.org/10.1111/j.1461-0248.2010.01570.x>, 2011.
- Pihlblad, J., Andresen, L. C., Macdonald, C. A., Ellsworth, D. S., and Carrillo, Y.: The influence of elevated CO<sub>2</sub> and soil depth on rhizosphere activity and nutrient availability in a mature *Eucalyptus* woodland, *Biogeosciences*, 20, 505–521, <https://doi.org/10.5194/bg-20-505-2023>, 2023.
- 1015 Piñeiro, J., Ochoa-Hueso, R., Drake, J. E., Tjoelker, M. G., and Power, S. A.: Water availability drives fine root dynamics in a *Eucalyptus* woodland under elevated atmospheric CO<sub>2</sub> concentration, *Functional Ecology*, 34, 2389–2402, <https://doi.org/10.1111/1365-2435.13660>, 2020.
- Prescott, C. E., Grayston, S. J., Helmisaari, H.-S., Kaštovská, E., Körner, C., Lambers, H., Meier, I. C., Millard, P., and Ostonen, I.: Surplus Carbon Drives Allocation and Plant–Soil Interactions, *Trends in Ecology & Evolution*, 35, 1110–1118, <https://doi.org/10.1016/j.tree.2020.08.007>, 2020.
- 1020 Reichert, T., Rammig, A., Fuchslueger, L., Lugli, L. F., Quesada, C. A., and Fleischer, K.: Plant phosphorus-use and -acquisition strategies in Amazonia, *New Phytologist*, 234, 1126–1143, <https://doi.org/10.1111/nph.17985>, 2022.
- Ross, G. M., Horn, S., Macdonald, C. A., Powell, J. R., Reynolds, J. K., Ryan, M. M., Cook, J. M., and Nielsen, U. N.: Metabarcoding mites: Three years of elevated CO<sub>2</sub> has no effect on oribatid assemblages in a *Eucalyptus* woodland, *Pedobiologia*, 81–82, 150667, <https://doi.org/10.1016/j.pedobi.2020.150667>, 2020.



- Schimel, J. P. and Weintraub, M. N.: The implications of exoenzyme activity on microbial carbon and nitrogen limitation in soil: a theoretical model, *Soil Biology and Biochemistry*, 35, 549–563, [https://doi.org/10.1016/S0038-0717\(03\)00015-4](https://doi.org/10.1016/S0038-0717(03)00015-4), 2003.
- Sistla, S. A., Rastetter, E. B., and Schimel, J. P.: Responses of a tundra system to warming using SCAMPS: a stoichiometrically coupled, acclimating microbe–plant–soil model, *Ecological Monographs*, 84, 151–170, <https://doi.org/10.1890/12-2119.1>, 2014.
- Sokol, N. W., Kuebbing, Sara. E., Karlsen-Ayala, E., and Bradford, M. A.: Evidence for the primacy of living root inputs, not root or shoot litter, in forming soil organic carbon, *New Phytologist*, 221, 233–246, <https://doi.org/10.1111/nph.15361>, 2019.
- Spohn, M.: Microbial respiration per unit microbial biomass depends on litter layer carbon-to-nitrogen ratio, *Biogeosciences*, 12, 817–823, <https://doi.org/10.5194/bg-12-817-2015>, 2015.
- Spohn, M., Ermak, A., and Kuzyakov, Y.: Microbial gross organic phosphorus mineralization can be stimulated by root exudates – A <sup>33</sup>P isotopic dilution study, *Soil Biology and Biochemistry*, 65, 254–263, <https://doi.org/10.1016/j.soilbio.2013.05.028>, 2013.
- Sun, L., Kominami, Y., Yoshimura, K., and Kitayama, K.: Root-exudate flux variations among four co-existing canopy species in a temperate forest, Japan, *Ecological Research*, 32, 331–339, <https://doi.org/10.1007/s11284-017-1440-9>, 2017.
- Sun, L., Ataka, M., Han, M., Han, Y., Gan, D., Xu, T., Guo, Y., and Zhu, B.: Root exudation as a major competitive fine-root functional trait of 18 coexisting species in a subtropical forest, *New Phytologist*, 229, 259–271, <https://doi.org/10.1111/nph.16865>, 2021.
- Sun, Z., Liu, S., Zhang, T., Zhao, X., Chen, S., and Wang, Q.: Priming of soil organic carbon decomposition induced by exogenous organic carbon input: a meta-analysis, *Plant Soil*, 443, 463–471, <https://doi.org/10.1007/s11104-019-04240-5>, 2019.
- Taneva, L., Pippen, J. S., Schlesinger, W. H., and Gonzalez-Meler, M. A.: The turnover of carbon pools contributing to soil CO<sub>2</sub> and soil respiration in a temperate forest exposed to elevated CO<sub>2</sub> concentration, *Global Change Biology*, 12, 983–994, <https://doi.org/10.1111/j.1365-2486.2006.01147.x>, 2006.
- Tang, J. Y. and Riley, W. J.: A total quasi-steady-state formulation of substrate uptake kinetics in complex networks and an example application to microbial litter decomposition, *Biogeosciences*, 10, 8329–8351, <https://doi.org/10.5194/bg-10-8329-2013>, 2013.
- Thum, T., Caldararu, S., Engel, J., Kern, M., Pallandt, M., Schnur, R., Yu, L., and Zaehle, S.: A new model of the coupled carbon, nitrogen, and phosphorus cycles in the terrestrial biosphere (QUINCY v1.0; revision 1996), *Geoscientific Model Development*, 12, 4781–4802, <https://doi.org/10.5194/gmd-12-4781-2019>, 2019.
- Turner, M. A., Caldararu, S., Engel, J., Rammig, A., and Zaehle, S.: Modelled forest ecosystem carbon–nitrogen dynamics with integrated mycorrhizal processes under elevated CO<sub>2</sub>, *Biogeosciences*, 21, 1391–1410, <https://doi.org/10.5194/bg-21-1391-2024>, 2024.
- Turner, B. L., Wells, A., and Condon, L. M.: Soil organic phosphorus transformations along a coastal dune chronosequence under New Zealand temperate rain forest, *Biogeochemistry*, 121, 595–611, <https://doi.org/10.1007/s10533-014-0025-8>, 2014.



- 1060 Vestergård, M., Reinsch, S., Bengtson, P., Ambus, P., and Christensen, S.: Enhanced priming of old, not new soil carbon at  
elevated atmospheric CO<sub>2</sub>, *Soil Biology and Biochemistry*, 100, 140–148, <https://doi.org/10.1016/j.soilbio.2016.06.010>, 2016.
- Walker, A. P., Zaehle, S., Medlyn, B. E., De Kauwe, M. G., Asao, S., Hickler, T., Parton, W., Ricciuto, D. M., Wang, Y.-P.,  
Wårlind, D., and Norby, R. J.: Predicting long-term carbon sequestration in response to CO<sub>2</sub> enrichment: How and why do  
current ecosystem models differ?, *Global Biogeochemical Cycles*, 29, 476–495, <https://doi.org/10.1002/2014GB004995>,  
1065 2015.
- Walker, A. P., De Kauwe, M. G., Medlyn, B. E., Zaehle, S., Iversen, C. M., Asao, S., Guenet, B., Harper, A., Hickler, T.,  
Hungate, B. A., Jain, A. K., Luo, Y., Lu, X., Lu, M., Luus, K., Megonigal, J. P., Oren, R., Ryan, E., Shu, S., Talhelm, A.,  
Wang, Y.-P., Warren, J. M., Werner, C., Xia, J., Yang, B., Zak, D. R., and Norby, R. J.: Decadal biomass increment in early  
secondary succession woody ecosystems is increased by CO<sub>2</sub> enrichment, *Nat Commun*, 10, 454,  
1070 <https://doi.org/10.1038/s41467-019-08348-1>, 2019.
- Walker, A. P., De Kauwe, M. G., Bastos, A., Belmecheri, S., Georgiou, K., Keeling, R. F., McMahon, S. M., Medlyn, B. E.,  
Moore, D. J. P., Norby, R. J., Zaehle, S., Anderson-Teixeira, K. J., Battipaglia, G., Brien, R. J. W., Cabugao, K. G., Cailleret,  
M., Campbell, E., Canadell, J. G., Ciais, P., Craig, M. E., Ellsworth, D. S., Farquhar, G. D., Fatichi, S., Fisher, J. B., Frank, D.  
C., Graven, H., Gu, L., Haverd, V., Heilman, K., Heimann, M., Hungate, B. A., Iversen, C. M., Joos, F., Jiang, M., Keenan,  
1075 T. F., Knauer, J., Körner, C., Leshyk, V. O., Leuzinger, S., Liu, Y., MacBean, N., Malhi, Y., McVicar, T. R., Penuelas, J.,  
Pongratz, J., Powell, A. S., Riutta, T., Sabot, M. E. B., Schleucher, J., Sitch, S., Smith, W. K., Sulman, B., Taylor, B., Terrer,  
C., Torn, M. S., Treseder, K. K., Trugman, A. T., Trumbore, S. E., van Mantgem, P. J., Voelker, S. L., Whelan, M. E., and  
Zuidema, P. A.: Integrating the evidence for a terrestrial carbon sink caused by increasing atmospheric CO<sub>2</sub>, *New Phytologist*,  
229, 2413–2445, <https://doi.org/10.1111/nph.16866>, 2021.
- 1080 Walker, T. W. and Syers, J. K.: The fate of phosphorus during pedogenesis, *Geoderma*, 15, 1–19, [https://doi.org/10.1016/0016-7061\(76\)90066-5](https://doi.org/10.1016/0016-7061(76)90066-5), 1976.
- Wang, Y. and Lambers, H.: Root-released organic anions in response to low phosphorus availability: recent progress,  
challenges and future perspectives, *Plant Soil*, 447, 135–156, <https://doi.org/10.1007/s11104-019-03972-8>, 2020.
- Wang, Y.-P., Huang, Y., Augusto, L., Goll, D. S., Helfenstein, J., and Hou, E.: Toward a Global Model for Soil Inorganic  
1085 Phosphorus Dynamics: Dependence of Exchange Kinetics and Soil Bioavailability on Soil Physicochemical Properties, *Global  
Biogeochemical Cycles*, 36, e2021GB007061, <https://doi.org/10.1029/2021GB007061>, 2022.
- Wieder, W. R., Cleveland, C. C., Smith, W. K., and Todd-Brown, K.: Future productivity and carbon storage limited by  
terrestrial nutrient availability, *Nature Geosci*, 8, 441–444, <https://doi.org/10.1038/ngeo2413>, 2015.
- Wutzler, T., Zaehle, S., Schumpf, M., Ahrens, B., and Reichstein, M.: Adaptation of microbial resource allocation affects  
1090 modelled long term soil organic matter and nutrient cycling, *Soil Biology and Biochemistry*, 115, 322–336,  
<https://doi.org/10.1016/j.soilbio.2017.08.031>, 2017.



- Wutzler, T., Yu, L., Schrumpf, M., and Zaehle, S.: Simulating long-term responses of soil organic matter turnover to substrate stoichiometry by abstracting fast and small-scale microbial processes: the Soil Enzyme Steady Allocation Model (SESAM; v3.0), *Geoscientific Model Development*, 15, 8377–8393, <https://doi.org/10.5194/gmd-15-8377-2022>, 2022.
- 1095 Yin, H., Li, Y., Xiao, J., Xu, Z., Cheng, X., and Liu, Q.: Enhanced root exudation stimulates soil nitrogen transformations in a subalpine coniferous forest under experimental warming, *Global Change Biology*, 19, 2158–2167, <https://doi.org/10.1111/gcb.12161>, 2013.
- Yu, L., Ahrens, B., Wutzler, T., Schrumpf, M., and Zaehle, S.: Jena Soil Model (JSM v1.0; revision 1934): a microbial soil organic carbon model integrated with nitrogen and phosphorus processes, *Geoscientific Model Development*, 13, 783–803, <https://doi.org/10.5194/gmd-13-783-2020>, 2020.
- 1100 Yu, L., Caldararu, S., Ahrens, B., Wutzler, T., Schrumpf, M., Helfenstein, J., Pistocchi, C., and Zaehle, S.: Improved representation of phosphorus exchange on soil mineral surfaces reduces estimates of phosphorus limitation in temperate forest ecosystems, *Biogeosciences*, 20, 57–73, <https://doi.org/10.5194/bg-20-57-2023>, 2023.
- Zaehle, S., Medlyn, B. E., De Kauwe, M. G., Walker, A. P., Dietze, M. C., Hickler, T., Luo, Y., Wang, Y.-P., El-Masri, B., Thornton, P., Jain, A., Wang, S., Warlind, D., Weng, E., Parton, W., Iversen, C. M., Gallet-Budynek, A., McCarthy, H., Finzi, A., Hanson, P. J., Prentice, I. C., Oren, R., and Norby, R. J.: Evaluation of 11 terrestrial carbon–nitrogen cycle models against observations from two temperate Free-Air CO<sub>2</sub> Enrichment studies, *New Phytologist*, 202, 803–822, <https://doi.org/10.1111/nph.12697>, 2014.
- 1105 Zerihun, A., McKENZIE, B. A., and Morton, J. D.: Photosynthate costs associated with the utilization of different nitrogen–forms: influence on the carbon balance of plants and shoot–root biomass partitioning, *New Phytologist*, 138, 1–11, <https://doi.org/10.1046/j.1469-8137.1998.00893.x>, 1998.
- Zhang, C., Cai, Y., Zhang, T., He, T., Li, J., Li, X., and Zhao, Q.: Litter removal increases the plant carbon input to soil in a *Pinus massoniana* plantation, *Eur J Forest Res*, 141, 833–843, <https://doi.org/10.1007/s10342-022-01476-2>, 2022.
- Zhang, H., Goll, D. S., Wang, Y.-P., Ciais, P., Wieder, W. R., Abramoff, R., Huang, Y., Guenet, B., Prescher, A.-K., Viscarra Rossel, R. A., Barré, P., Chenu, C., Zhou, G., and Tang, X.: Microbial dynamics and soil physicochemical properties explain large-scale variations in soil organic carbon, *Global Change Biology*, 26, 2668–2685, <https://doi.org/10.1111/gcb.14994>, 2020.
- 1115 Zhou, J., Wen, Y., Shi, L., Marshall, M. R., Kuzyakov, Y., Blagodatskaya, E., and Zang, H.: Strong priming of soil organic matter induced by frequent input of labile carbon, *Soil Biology and Biochemistry*, 152, 108069, <https://doi.org/10.1016/j.soilbio.2020.108069>, 2021.